AWARD NUMBER: W81XWH-17-1-0291

TITLE: Modeling Human Gamma Delta T Cells as Antitumor Agents In Vivo

PRINCIPAL INVESTIGATOR: Jenny Gumperz, PhD

CONTRACTING ORGANIZATION: University of Wisconsin System
Madison, WI 53715

REPORT DATE: August 2018

TYPE OF REPORT: Annual

PREPARED FOR: U.S. Army Medical Research and Materiel Command
Fort Detrick, Maryland 21702-5012

REPORT DOCUMENTATION PAGE

Form Approved
OMB No. 0704-0188

1. REPORT DATE	2. REPORT TYPE	3. DATES COVERED
August 2018	Annual	1 Aug 2017 - 31 Jul 2018

4. TITLE AND SUBTITLE
Modeling Human Gamma Delta T Cells as Antitumor Agents In Vivo

5a. CONTRACT NUMBER

5b. GRANT NUMBER
W81XWH-17-1-0291

5c. PROGRAM ELEMENT NUMBER

6. AUTHOR(S)
Jenny E. Gumperz, PhD

E-Mail: jegumperz@wisc.edu

5d. PROJECT NUMBER

5e. TASK NUMBER

5f. WORK UNIT NUMBER

7. PERFORMING ORGANIZATION NAME(S) AND ADDRESS(ES)

University of Wisconsin System
21 N PARK ST STE 6401
MADISON, WI 53715-1218

8. PERFORMING ORGANIZATION REPORT NUMBER

9. SPONSORING / MONITORING AGENCY NAME(S) AND ADDRESS(ES)
USA Med Research ACQ Activity
U.S. Army Medical Research and Materiel Command
Fort Detrick, Maryland 21702-5012

10. SPONSOR/MONITOR'S ACRONYM(S)

11. SPONSOR/MONITOR'S REPORT NUMBER(S)

12. DISTRIBUTION / AVAILABILITY STATEMENT

Approved for Public Release; Distribution Unlimited

13. SUPPLEMENTARY NOTES

14. ABSTRACT
The central objective of this project is to provide mechanistic data that will support the development of human Vγ9Vδ2 T cells as an anti-tumor cellular immunotherapy for lymphomas driven by Epstein-Barr virus (EBV) infection. During this research period we have completed the following: i) Obtained local IRB and ACUC approvals and obtained HRPO and ACURO approval; ii) obtained adult human peripheral blood cells, expanded Vγ9Vδ2 T cells, sorted to obtain high-purity preparations, generated frozen stocks and confirmed viability upon thaw; iii) generated viral stocks and performed in vivo dose-response experiments to determine appropriate dosing for lymphoma formation; iv) initiated analyses to identify an appropriate BTN3A1 blocking mAb; v) resolved technical issues that caused lysis of cord blood cells prior to injection into immune-deficient mice and failure of the human immune cells to successfully engraft after injection. We are thus now in a position where we will be able to move forward with performing the proposed mechanistic experiments.

15. SUBJECT TERMSAACURO
Epstein-Barr virus (EBV); B cell lymphoma; γδ T cell; cellular immunotherapy; humanized mouse; umbilical cord blood.

16. SECURITY CLASSIFICATION OF:			17. LIMITATION OF ABSTRACT	18. NUMBER OF PAGES	19a. NAME OF RESPONSIBLE PERSON
a. REPORT	b. ABSTRACT	c. THIS PAGE			USAMRMC
U Unclassified	U Unclassified	U Unclassified	UU Unclassified	50	19b. TELEPHONE NUMBER *(include area code)*

Table of Contents

Page

1. **Introduction…….1**
2. **Keywords…….1**
3. **Accomplishments……..……...1-4**
4. **Impact……...……4-5**
5. **Changes/Problems...…….5-6**
6. **Products……..……..…….6-7**
7. **Participants & Other Collaborating Organizations……7-8**
8. **Special Reporting Requirements……9**
9. **Appendices……10-48**

1. **INTRODUCTION:** The central objective of this project is to provide mechanistic data that will support the development of human γδ T cells as an anti-tumor cellular immunotherapy for lymphomas driven by Epstein-Barr virus (EBV) infection. The project employs a humanized mouse model, in which highly immunodeficient mice are injected with human umbilical cord blood cells that were briefly exposed *in vitro* to EBV. Over the ensuing three weeks, the human immune cells (including both T and B lymphocytes) expand *in vivo*, and human B cell lymphomas form in the fatty tissue surrounding peritoneal organs. The B cell lymphomas are infiltrated by autologous T cells, but these are suppressed by inhibitory ligands and fail to control the cancer. We have recently shown that administration of human γδ T cells ($V\gamma9V\delta2^+$ T cells) that were expanded *in vitro* from peripheral blood of unrelated healthy adult donors is highly effective at reducing the tumor burden in this model. Thus, in contrast to the endogenous T lymphocytes, the immunotherapeutic γδ T cells appear to avoid becoming suppressed by the existing inhibitory pathways (please see our recently published paper included in Appendix for more information). The two Specific Aims of this project focus on investigating the nature of the activation signals required for the immunotherapeutic effects of the γδ T cells. Specifically, Aim 1 investigates the requirement for stimulation via T cell receptor (TCR)-mediated recognition of butyrophilin (BTN3A1) molecules that associate with lipid metabolites such as isopentenyl pyrophosphate (IPP). Aim 2 investigates the role of activation mediated by an "NK" receptor called NKG2D, that is expressed by $V\gamma9V\delta2^+$ T cells. The information gained from these studies will allow us to identify human lymphoma patients who are likely to fulfill the requirements for $V\gamma9V\delta2^+$ T cell activation, in that their lymphomas present the required activating signals. This will allow us to proceed with setting up a pilot clinical trial to test this therapeutic approach.

2. **KEYWORDS:** Epstein-Barr virus (EBV); B cell lymphoma; γδ T cell; cellular immunotherapy; humanized mouse; umbilical cord blood.

3. **ACCOMPLISHMENTS:**
   - **What were the major goals of the project?**

Specific Aim 1: **Use human EBV-driven lymphomagenesis model to test the impact of TCR-mediated activation of $V\gamma9V\delta2^+$ T cells on their anti-tumor effects *in vivo*.**	**Expected timeline (months)**	**Completion status**
Major Task 1: **Perform in vivo blocking experiments to test requirement for recognition of BTN3A1 protein by adoptively transferred γδ T cells**	**9**	**50%**
Prior to award: Local IRB/IACUC Approval	0	100%
Subtask 1: Obtain HRPO approval for obtaining and using human peripheral blood samples from healthy adult volunteers, and for acquiring de-identified human umbilical cord blood samples from commercial sources	1-2	100%
Subtask 2:	1-2	100%

Obtain ACURO approval for experimental use of immune deficient mice		
Milestone Achieved: HRPO/ACURO Approval	**2**	**100%**
Subtask 3: Expand human Vγ9Vδ2$^+$ T cells from adult peripheral blood samples and make sterile frozen aliquots	2	100%
Subtask 4: Test different anti-BTN3A1 mAb clones to identify one or more that provide good blocking of Vγ9Vδ2$^+$ T cell responses *in vitro*. Also identify and test isotype control mAb.	2	60%
Subtask 5: Generate viral stock	1-2	100%
Subtask 6: Perform preliminary experiment to titrate viral dose required for visible tumor formation within 30 days	2	100%
Subtask 7: Perform preliminary experiments using umbilical cord blood engrafted mice to test selected anti-BTN3A1 mAbs (vs. isotype control) for half-life in serum, binding to target cells *in vivo*, and whether cells become depleted by the specific anti-BTN3A1 mAb.	3	0%
Subtask 8: Engraft mice with EBV-exposed human umbilical cord cells	3-4	0%
Subtask 9: Administer γδ T cell adoptive therapy or PBS, in the presence of anti-BTN3A1 blocking or isotype mAb (4 groups of 6 mice each).	4	0%
Subtask 10: Sacrifice mice; weigh tumors; collect and preserve tissues for IHC; collect tissues, isolate cells, freeze samples for later flow cytometric analysis.	4	0%
Subtask 11: Perform fluorescent mAb staining for human T and B lymphocytes, and for their expression of molecules indicating activation or functional status; run samples on flow cytometer.	4	0%
Subtask 12: Determine appropriate gating strategies and analyze flow cytometry data.	4	0%
Subtask 13: Prepare tissue blocks, cut serial sections, and make slides for IHC.	4	0%
Subtask 14: Perform IHC staining for human and viral antigens.	4-5	0%

Subtask 15: Perform microscopic analysis of IHC slides and take photographs of relevant fields.	5-6	0%

Subtask 16: Perform analysis of microscopy pictures using imaging software to generate quantitative results.	6	0%
Subtask 17: Repeat Subtasks 8-16.	4-7	0%
Subtask 18: Repeat Subtasks 8-16 again.	5-8	0%
Milestone(s) Achieved: **Information on whether TCR-mediated activation is required**	**9**	**50%**
Major Task 2: **Use pharmacological inhibitors (e.g. statins) to inhibit production of IPP**	**8-16**	**10%**
Subtask 1: Expand human Vγ9Vδ2$^+$ T cells from adult peripheral blood samples and make sterile frozen aliquots	8	100%
Subtask 2: Perform preliminary optimizing experiments using EBV-exposed umbilical cord blood engrafted mice to test dosing and off-target effects of administering statins.	8-9	0%
Subtask 3: Confirm ability of selected statin to inhibit Vγ9Vδ2$^+$ T cell responses to BTN3A1$^+$ target cells *in vitro.*	9	100%
Subtask 4: Engraft mice with EBV-exposed human umbilical cord cells	9-10	0%
Subtask 5: Administer γδ T cell adoptive therapy or PBS, in the presence of statin or vehicle (4 groups of 6 mice each).	10	0%
Subtask 6: Sacrifice mice; weigh tumors; collect and preserve tissues for IHC; collect tissue, isolate cells, freeze samples for later flow cytometric analysis.	10	0%
Subtask 7: Perform flow cytometry and IHC assessment as in Major Task 1 subtasks 11-16	10	0%
Subtask 8: Repeat Subtasks 4-7.	11-14	0%

Subtask 9: Repeat Subtasks 4-7 again.	12-15	0%
Milestone(s) Achieved: **Information on whether IPP production is required.**	**16**	**5%**

- **What was accomplished under these goals?**
  - 1) The major activities designated for this period of the grant were as follows: *i*) to gain regulatory approvals required for the project; *ii*) obtain human blood samples and expand γδ T cells so as to generate frozen aliquots of immunotherapy cells to be used in subsequent experiments; *iii*) generate and test viral stocks to be stored frozen and used in subsequent experiments; *iv*) set up experiment to test role of butyrophilin (BTN3A1) protein; *v*) perform analyses to determine outcome of BTN3A1 experiment; *vi*) start experiment to test role of isopentenylpyrophosphate (IPP), the main endogenous ligand for BTN3A1.
  - 2) The specific objectives were to gain information on the importance of BTN3A1 and IPP for the immunotherapeutic effects of γδ T cells in this model.
  - 3) The key outcomes are that we have successfully completed the supporting tasks required so that we will be able to perform the proposed experiments (items *i-iii* of the major activities; item *iv* is partially completed). However, due to technical difficulties arising from unexpected changes in the properties of the human umbilical cord blood samples used to establish the experimental model (discussed in greater detail below in section 5), we have not yet performed the central experiments or the associated analyses. Importantly, we believe we have now identified solutions to these technical difficulties, and expect to now be able to make progress towards completing the proposed experiments.
- **What opportunities for training and professional development has the project provided?**
  - Dr. Jenny Gumperz Ph.D. and Dr. Dana Baiu Ph.D. each provided one-on-one training to undergraduate students in association with this project: Dr. Gumperz trained a student (Ms. Isabel Monti) in techniques involved in performing immunohistochemistry (IHC) on tissue sections from humanized mice and on how to analyze the resulting slides; Dr. Baiu trained two students (Mr. Matthew Dandan and Ms. Maegan Sheehan) in techniques relating to purifying monoclonal antibodies from hybridoma cells, testing to confirm their specificity, and fluorescently labeling them for use in flow cytometry. Dr. Baiu also engaged in Professional Development activities by attending the International Conference on EBV and KSHV 2018, which took place at the University of Wisconsin in July 2018.
- **How were the results disseminated to communities of interest?**
  - Nothing to Report.
- **What do you plan to do during the next reporting period to accomplish the goals?**
  - We expect to proceed with the items outlined in the approved Statement of Work.

4. **IMPACT:**
   - **What was the impact on the development of the principal discipline(s) of the project?**

- Nothing to Report.

- **What was the impact on other disciplines?**
  - Nothing to Report.

- **What was the impact on technology transfer?**
  - Nothing to Report.

- **What was the impact on society beyond science and technology?**
  - Nothing to Report.

5. **CHANGES/PROBLEMS:**

- **Changes in approach and reasons for change**
  - Nothing to Report.

- **Actual or anticipated problems or delays and actions or plans to resolve them**
  - During this reporting period, we encountered two significant technical problems related to the human umbilical cord blood samples used to establish our humanized mouse model of EBV-driven lymphoma. The first problem was that the cord blood cell samples that we obtained from a commercial supplier (AllCells Inc.) often underwent severe cell lysis during the viral exposure step of our protocol, preventing us from being able to set up our *in vivo* experiments. This problem had seldom if ever arisen in the 3 years that we had carried out similar experiments prior to this reporting period, and we suspected it was caused by a change in the cord blood purification protocol used by the commercial supplier. We thus arranged to obtain totally de-identified human umbilical cord blood from other sources, and began purifying the mononuclear cells ourselves using Ficoll density gradient centrifugation. After taking this step, we found that only about one third of the samples lysed upon viral exposure, and we determined that the lysis was associated with the presence of high levels of immature neutrophils that had co-purified with the cord blood mononuclear cells. We established that by using magnetic-bead sorting to remove neutrophils, we are able to prevent lysis of the sample during virus exposure.
  - After solving the lysis problem, we became aware that many of the cord blood samples now failed to yield human engraftment that lasted more than one week in the NSG mice. After further analysis, we determined that the failure to engraft was associated with the presence of high numbers of nucleated red blood cells that were not removed by the density gradient centrifugation. Based on our own observations and on data from the published literature, we believe that when human cell samples containing a high percentage of red blood cells are injected into the mice, glycans on the human red blood cells activate murine phagocytic cells, leading to the rapid elimination of *all* of the human cells. Importantly, we have been able to resolve this problem by using magnetic-bead sorting to remove red blood cells, and have established that we are now again able to generate lasting human immune engraftment that gives rise to EBV-driven lymphomas in the mice. Thus, although these two technical problems cost us several months of trouble-shooting time, we are now in a position to move forward with the proposed studies to assess pathways required for the therapeutic activity of allogeneic human γδ T cells.
  - The central remaining concern is that we are now typically obtaining fewer cord blood mononuclear cells from each cord blood sample than we originally expected (which

means we will need to reduce the number of mice per experimental group and carry out more repeat experiments). From discussions with colleagues in UW's OB/Gyn department, we have concluded that the biological differences we have noted in the human umbilical cord samples may be due to changes in birthing practices (e.g. delayed clamping of umbilical cords) that are becoming widespread throughout hospitals in the U.S., and therefore may not be fully resolved by switching to a different supplier of cord blood.

- Hence, we are now planning to explore whether we can generate a similar *in vivo* EBV-lymphomagenesis model using samples obtained from human adults. These will either be discarded remnants of adult human G-CSF mobilized blood preparations that were generated for clinical hematopoietic transplantation, or cells obtained from cadaveric splenic tissue from individuals who had opted to donate their organs for transplantation after death. Based on our findings from a separate project where we have engrafted NSG mice with such adult human cells, we expect that generating the EBV-lymphoma model will be feasible. The approach of using cells from these sources has several key advantages, including the following: *i*) these sources may provide enough cells to perform multiple experiments in sequence, which may reduce our inter-experimental variability (this in turn may reduce the number of times each experiment needs to be independently repeated); *ii*) the use of adult cells to generate the model means the model will more closely reflect human therapeutic situations.

- **Changes that had a significant impact on expenditures**
  - It took slightly longer than expected to recruit the scientist who is performing these studies, and therefore she did not begin working on the project until the third month of the reporting period. Additionally, due to the technical problems noted above, we were not able to perform as many *in vivo* experiments as expected and thus spent less than expected on mice and supplies.

- **Significant changes in use or care of human subjects, vertebrate animals, biohazards, and/or select agents**
  - Nothing to Report.

6. **PRODUCTS:**

- **Publications, conference papers, and presentations**
  - **Journal publications.** Nothing to Report
  - **Books or other non-periodical, one-time publications.** We have authored a chapter ("Expansion and Adoptive Transfer of Human Vδ2$^+$ T cells to Assess Antitumor Effects In Vivo", by Akshat Sharma, Nicholas Zumwalde, and Jenny E. Gumperz) that is slated to be published in: Methods in Molecular Biology: Cancer Immunosurveillance, Eds Alejandro Lopez-Soto and Alicia Folgueras, Springer-Verlag New York).
  - **Other publications, conference papers, and presentations.** Conference presentation: Gumperz JE, Keynote presentation entitled "Investigating anti-tumor functions of human innate T lymphocytes in vivo", given at the Center for Immunology and Immune-based Diseases, Carver College of Medicine, University of Iowa's 7th Annual Retreat, August 16, 2018.

- **Website(s) or other Internet site(s)**
  Methods in Molecular Biology website for book containing our chapter, referenced above:
  https://www.springer.com/gp/book/9781493988846

- **Technologies or techniques**
  See above website.

- **Inventions, patent applications, and/or licenses**
  Nothing to Report.

- **Other Products**
  Nothing to Report.

7. PARTICIPANTS & OTHER COLLABORATING ORGANIZATIONS

- **What individuals have worked on the project?**

Name:	Jenny E. Gumperz, Ph.D.
Project Role:	Principal Investigator
Researcher Identifier (e.g. ORCID ID):	0000-0003-1852-2192
Nearest person month worked:	4
Contribution to Project:	Dr. Gumperz oversees all aspects of the project to ensure that the proposed goals are accomplished. These activities include the design of experiments, analysis and interpretation of the data, budget oversight, and manuscript and progress report preparation.
Funding Support:	National Institutes of Health.
Name:	Dana C. Baiu, Ph.D.
Project Role:	Associate Scientist
Researcher Identifier (e.g. ORCID ID):	N/A
Nearest person month worked:	8
Contribution to Project:	Conducts experiments and analyses; interprets, analyzes, and summarizes data.
Funding Support:	
Name:	Akshat Sharma, M.S.
Project Role:	Graduate student

Researcher Identifier (e.g. ORCID ID):	0000-0002-2632-2935
Nearest person month worked:	1
Contribution to Project:	Prepared reagents, conducted experiments
Funding Support:	National Institutes of Health.
Name:	Nicholas A. Zumwalde, Ph.D.
Project Role:	Postdoctoral Fellow
Researcher Identifier (e.g. ORCID ID):	0000-0003-3786-7735
Nearest person month worked:	1
Contribution to Project:	Prepared reagents, conducted experiments
Funding Support:	American Cancer Society
Name:	Shannon C. Kenney
Project Role:	Collaborator
Researcher Identifier (e.g. ORCID ID):	N/A
Nearest person month worked:	1
Contribution to Project:	Generates virus stocks and provides expertise on aspects of experimental analyses and interpretation.
Funding Support:	National Institutes of Health.

- **Has there been a change in the active other support of the PD/PI(s) or senior/key personnel since the last reporting period?**
  - A previously active grant ("The role of invariant natural killer T cells in HIV-1 cell-to-cell transmission") was closed out.
  - The PI was awarded a new NIH grant (R01AI136500 "Mechanisms of iNKT cell anti-viral adjuvancy") that started on Aug 7th, 2018.
- **What other organizations were involved as partners?**
  - Nothing to Report.

8. **SPECIAL REPORTING REQUIREMENTS**
    - **COLLABORATIVE AWARDS:** Not applicable.
    - **QUAD CHARTS:** Not applicable.

9. **APPENDICES:** Copy of journal article (Zumwalde et al., *JCI Insight* 2017) that describes methodologies and principal findings upon which this award was based. Copy of book chapter (Sharma et al., *Methods in Molecular Biology*) that is slated to be published in early 2019 and that describes the model system and methods used in this project.

JCI insight

RESEARCH ARTICLE

Adoptively transferred Vγ9Vδ2 T cells show potent antitumor effects in a preclinical B cell lymphomagenesis model

Nicholas A. Zumwalde,[1] Akshat Sharma,[1] Xuequn Xu,[1] Shidong Ma,[2] Christine L. Schneider,[3] James C. Romero-Masters,[2] Amy W. Hudson,[3] Annette Gendron-Fitzpatrick,[4] Shannon C. Kenney,[2] and Jenny E. Gumperz[1]

[1]Department of Medical Microbiology and Immunology, [2]Department of Oncology, University of Wisconsin School of Medicine and Public Health, Madison, Wisconsin, USA. [3]Department of Microbiology and Molecular Genetics, Medical College of Wisconsin, Milwaukee, Wisconsin, USA. [4]Comparative Pathology Laboratory, Research Animal Resources Center, University of Wisconsin School of Medicine and Public Health, Madison, Wisconsin, USA.

A central issue for adoptive cellular immunotherapy is overcoming immunosuppressive signals to achieve tumor clearance. While γδ T cells are known to be potent cytolytic effectors that can kill a variety of cancers, it is not clear whether they are inhibited by suppressive ligands expressed in tumor microenvironments. Here, we have used a powerful preclinical model where EBV infection drives the de novo generation of human B cell lymphomas in vivo, and autologous T lymphocytes are held in check by PD-1/CTLA-4–mediated inhibition. We show that a single dose of adoptively transferred Vδ2$^+$ T cells has potent antitumor effects, even in the absence of checkpoint blockade or activating compounds. Vδ2$^+$ T cell immunotherapy given within the first 5 days of EBV infection almost completely prevented the outgrowth of tumors. Vδ2$^+$ T cell immunotherapy given more than 3 weeks after infection (after neoplastic transformation is evident) resulted in a dramatic reduction in tumor burden. The immunotherapeutic Vδ2$^+$ T cells maintained low cell surface expression of PD-1 in vivo, and their recruitment to tumors was followed by a decrease in B cells expressing PD-L1 and PD-L2 inhibitory ligands. These results suggest that adoptively transferred PD-1^{lo} Vδ2$^+$ T cells circumvent the tumor checkpoint environment in vivo.

Introduction

γδ T cells are attractive candidates for adoptive immunotherapy in human cancer patients because they mediate potent antitumor effects in an MHC-independent manner (1–4), and therefore they do not require HLA matching of donors and recipients. Physiologically, γδ T cells are thought to be important for immunosurveillance (i.e., eradication of nascently transformed cells), since they can recognize early danger signals associated with neoplastic changes (5, 6). However, their role in controlling established tumors is not clear, as recent studies have identified tumor-infiltrating γδ T cells that appear to have protumorigenic functions (7, 8). Critical questions about the use of γδ T cells as agents of cellular immunotherapy thus involve understanding whether their ability to control cancers is subject to changes associated with tumor maturation, including whether their activating ligands are maintained or downregulated during the progression of tumorigenesis, and whether their responses are controlled by suppressive ligands that become upregulated during tumorigenesis.

Human γδ T cells are divided into 2 main subsets based on whether their T cell receptors (TCRs) use the Vδ1 or Vδ2 chain. Vδ1$^+$ T cells are mainly found in epithelial tissues, while most of the γδ T cells in human blood use the Vδ2 chain in combination with the Vγ9 chain (9). The mechanisms responsible for activating Vδ2$^+$ T cells are better understood than those of Vδ1$^+$ T cells, and therefore the Vδ2$^+$ subset has been more extensively investigated for immunotherapy. Functional responses of Vδ2$^+$ T cells can be initiated by at least 3 distinct recognition pathways: (a) via the TCR, (b) via natural killer (NK) family receptors such as NKG2D, and (c) via Fc receptor (CD16) binding to antibody-coated target cells (10). Each of these pathways may facilitate their antitumor responses.

TCR responses of Vδ2$^+$ cells depend on target cell expression of a highly conserved cell surface protein called butyrophilin 3A1 (BTN3A1), which is normally expressed in all tissues (11, 12). However, Vδ2$^+$

Authorship note: N.A. Zumwalde, A. Sharma, and X. Xu contributed equally to this work.

Conflict of interest: The authors have declared that no conflict of interest exists.

Submitted: February 1, 2017
Accepted: May 31, 2017
Published: July 6, 2017

Reference information:
JCI Insight. 2017;2(13):e93179. https://doi.org/10.1172/jci.insight.93179.

TCRs only recognize the BTN3A1 molecule after it has undergone structural changes resulting from association with specific isoprenoid lipids (13–16). Isoprenoid lipids that activate Vδ2$^+$ T cells include prenylpyrophosphate metabolites that are produced by many bacterial species (17), as well as an intermediate of the mevalonate pathway called isopentenylpyrophosphate (IPP) that is produced by eukaryotic cells. Activity of the mevalonate pathway is often upregulated during neoplastic transformation, which in turn can result in greater accumulation of the IPP intermediate in cancer cells compared with normal cells. The presence of high levels of IPP appears to be a key factor in the ability of Vδ2$^+$ T cells to respond to human cancer cells in vitro (18). However, it is not clear whether endogenous expression levels of this metabolic intermediate are sufficient to permit immunotherapeutic Vδ2$^+$ T cells to target emerging or established cancers in vivo.

γδ T cells may also specifically target tumors in a TCR-independent manner through recognition of innate ligands. Vδ2$^+$ T cells express an activating receptor of the NK complex called NKG2D. This is a transmembrane C-type lectin that recognizes at least 8 different ligands, including the MHC class I–related chain (MIC) A and B molecules, and a family of related molecules called UL16-binding protein (ULBP) 1–6 (19). Expression of MICA/B and ULBP molecules is increased under conditions of stress (e.g., microbial infection, hyperproliferation, and neoplastic transformation), and many tumors express elevated levels of these ligands at the cell surface (20). NKG2D-mediated recognition of MICA/B molecules markedly costimulates TCR-dependent effector responses of Vδ2$^+$ T cells, and may also be sufficient to activate them in a TCR-independent manner (21–23). However, ligands recognized by NKG2D can be downregulated from the cell surface by tumor cells and secreted in a soluble form as a mechanism of immune evasion or suppression (24), and therefore the use of this recognition pathway for immunotherapy must be carefully evaluated.

Preclinical in vivo modeling is thus key to understanding how to design effective immunotherapy strategies using human γδ T cells. However, a challenge to modeling the actions of human Vδ2$^+$ T cells in vivo is that rodents do not possess a similar isoprenoid-reactive γδ T cell subset, and lack the BTN3A1 isoform (25, 26). Prior studies have thus xenografted established human tumors into immune-deficient mice in the presence or absence of human Vδ2$^+$ T cells to evaluate their effects in vivo (27–32). These studies have provided important demonstrations of the antitumor potential of human Vδ2$^+$ T cells. However, studies of this kind do not capture the dynamic changes associated with the process of tumorigenesis, and in particular may not model how the upregulation of immunosuppressive ligands by tumors, which is accompanied by the presence of anergized T lymphocytes, affects the success of cellular immunotherapy.

Here we have used a powerful model in which Epstein-Barr virus (EBV) drives human B cells to transition from healthy cells into lymphomas over the course of several weeks in vivo. EBV is a human-specific γ-herpesvirus that is associated with several types of human B cell lymphoma, including Burkitt lymphoma, Hodgkin lymphoma, diffuse large B cell lymphoma, and posttransplant lymphoproliferative disease (33). A key feature of our model system is that neoplastic transformation of the human B cells occurs in the presence of autologous human T lymphocytes (34). Importantly, the autologous T cells are held in check by PD-1 and CTLA-4, which limit their ability to control the B lymphomas (35). This system therefore allowed us to test the effects of Vδ2$^+$ T cell adoptive immunotherapy in vivo before and after the establishment of tumor masses, and in the context of tumor-suppressive ligands.

Results

De novo lymphomagenesis. To induce the formation of human B cell lymphomas in vivo, we briefly incubated human umbilical cord blood mononuclear cells (CBMCs) with EBV in vitro to allow viral attachment to the B cells, and then injected the human cells intraperitoneally into NSG mice (34). Using this protocol, typically about 90% of the mice develop tumors that result in mortality within 5 weeks (Figure 1A). Histological analysis revealed that by 14 days after injection, lymphoid aggregates are apparent in the fatty tissue near the pancreas. The aggregates include cells expressing the EBV nuclear antigen 1 (EBNA1), indicating that virally infected cells are present, but at this stage signs of neoplastic transformation are not apparent (Figure 1B). However, by 21 days after injection the lymphoid aggregates do show signs of neoplasia, including the presence of mitotic figures, areas of necrosis, and apoptotic debris (Figure 1B). By 28 days after injection, the lymphoid masses have expanded dramatically and typically appear to have started invading nearby organ tissue (Figure 1B). Based on these results, administration of cellular immunotherapy during the first week after injection of the EBV-treated CBMCs will likely assess immunosurveillance effects (i.e., clearance of EBV-infected cells prior to generation of a tumor microenvironment), whereas administering the immunotherapy later than 3 weeks after injection will assess the impact on established tumors.

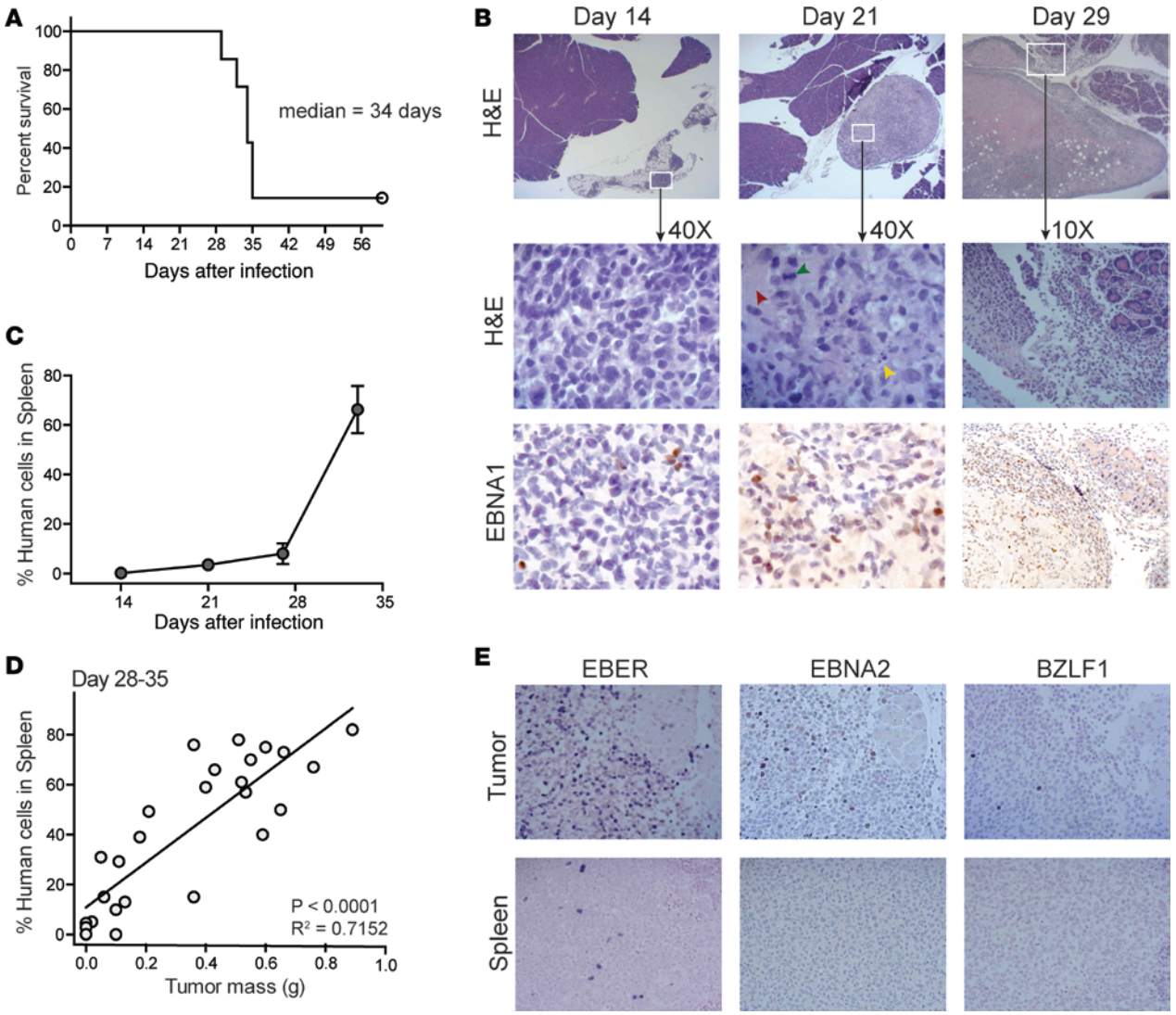

Figure 1. Model of human EBV-driven lymphomagenesis. Human umbilical cord blood mononuclear cells (CBMCs) were exposed to EBV for 2 hours in vitro and then washed, and 10×10^6 cells per mouse were injected intraperitoneally into NSG mice. (**A**) Survival results from a representative experiment with 7 mice; similar results were obtained in a second independent experiment. (**B**) Histological analyses of peri-pancreatic tissue taken at the indicated times after injection of the human cells. Top row shows low magnification (×2) H&E–stained images revealing the growth of lymphoid masses near pancreatic tissue. Middle row shows higher magnification of the indicated areas; neoplastic changes are visible at the day 21 time point, including areas of necrosis (red arrowhead), apoptotic debris (yellow arrowhead), and mitotic figures (green arrowhead). The bottom row shows IHC staining to detect expression of the EBNA1 viral protein (visualized with diaminobenzidine, brown color). The sections are counterstained with hematoxylin (blue color). (**C**) Frequency of human cells in spleen as determined by flow cytometric analysis of total splenocytes at the indicated time points. Each symbol represents the mean frequency from 3 different mice; error bars (not always visible on this scale) show the standard deviations. (**D**) The frequency of human cells in spleen was plotted against the total mass of tumor tissue excised from the peritoneal cavity for each mouse. Results are from mice sacrificed between 28 and 35 days after injection of EBV-treated CBMCs. Statistical results from a linear regression analysis are shown in the bottom-right corner of the plot. (**E**) Histological analyses for indicators of EBV infection from tumor tissue (top row) and spleen tissue (bottom row) at ×20 magnification. Left panels show in situ hybridization for EBV-encoded small RNAs (EBER, indicated by dark purple color); middle and right panels show IHC staining for the EBV proteins EBNA2 and BZLF1, respectively (positive cells have dark nuclei).

Spleen appears protected from tumorigenesis. Analysis of human cells in the spleens of mice engrafted with EBV-treated CBMCs consistently showed that there was a slow increase in human cell frequency between 14 and 28 days after injection, followed by a rapid rise between day 28 and 35 (Figure 1C). There was a clear correlation between the frequency of human cells in the spleen and the mass of the peritoneal tumors during the day 28–35 time window (Figure 1D), suggesting that tumorigenesis is associated with expansion of human cells in the spleen. However, unlike lymphoid masses in the peritoneal cavity, there was no histological evidence of neoplasia in the spleen (data not shown). Tumors in the peritoneal cavity contained abundant cells expressing EBV-encoded small RNAs (EBERs), as well as proteins associated with type-III EBV latency (EBNA2) and

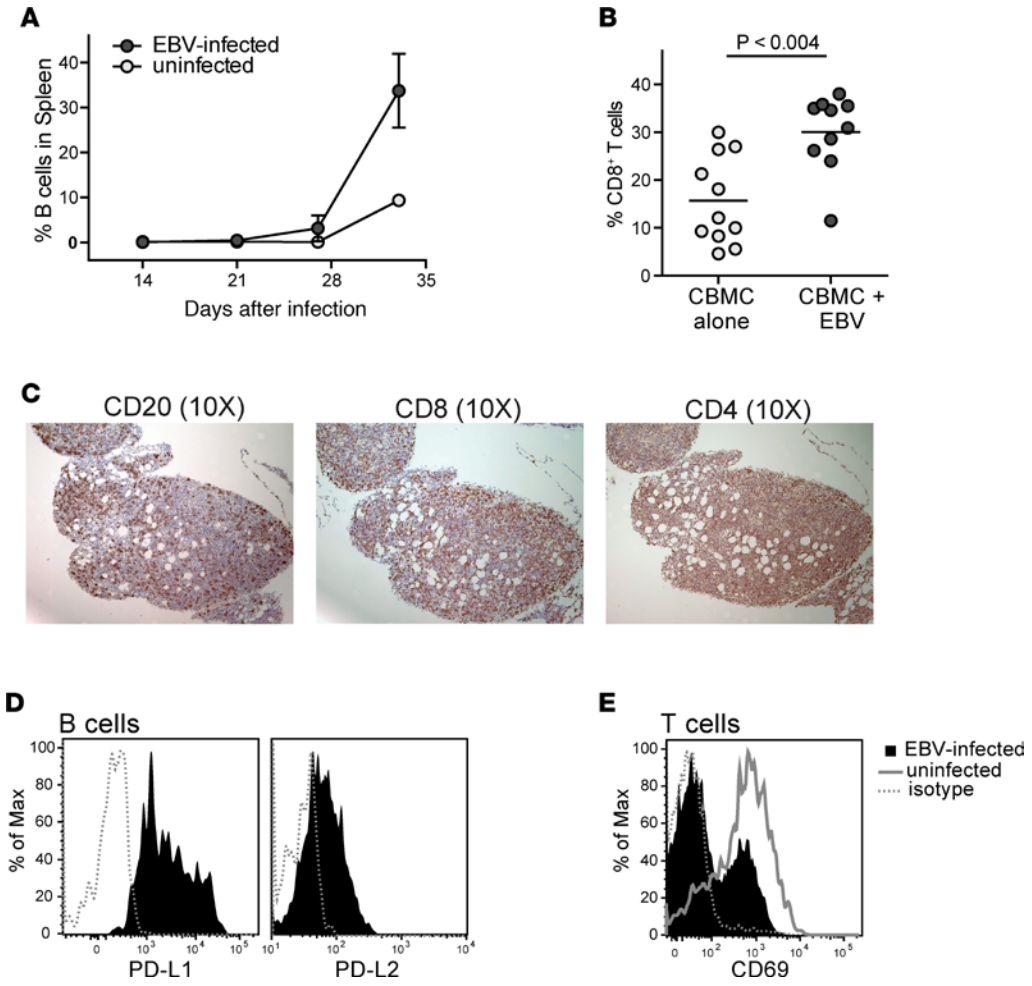

Figure 2. Autologous T cells are expanded during EBV infection. NSG mice were injected with 10 × 10^6 EBV- or mock-treated (uninfected) human umbilical cord blood mononuclear cells (CBMCs). (**A**) Plot showing the percentage of the human cells from spleen that stained positively for the B cell marker CD19 at the indicated time points after injection. Each data point represents the mean from 3 different mice; error bars (not always visible on this scale) show the standard deviations. (**B**) Percentage of $CD8^+$ T cells of the human cells in spleens harvested between 26 and 35 days after injection. Each data point shows the results from an individual mouse. The *P* value was calculated using a 2-tailed nonparametric *t* test (Mann-Whitney analysis). (**C**) IHC of serial sections of a peritoneal tumor taken at 3 weeks after injection of EBV-treated CBMCs. Brown color shows staining for human CD20 (left), human CD8 (middle), and human CD4 (right); hematoxylin counterstaining shows cell nuclei (blue color). (**D**) Flow cytometric analysis of tumor B cells for PD-L1 (left) and PD-L2 (right). Filled histograms show staining by specific mAbs, dotted line shows staining by an isotype control mAb. (**E**) Flow cytometric analysis of splenic T cells from an EBV-infected mouse for expression of the activation marker CD69 (filled histogram) compared to an isotype control mAb (dotted line); the solid gray line shows CD69 staining of splenic T cells from an uninfected mouse.

lytic replication (BZLF1) (Figure 1E), suggesting a high level of viral transforming activity in the tumors. In contrast, the spleen showed only sparse EBER staining and little or no positive staining for EBNA2 or BZLF1. Thus, although virally infected cells are present in the spleen, they are likely in a deeper state of latency, and neoplastic transformation resulting in the formation of tumors is limited or absent at this location.

Expansion of autologous T cells during EBV infection. The human CBMC samples used to engraft the mice for these studies typically contain less than 10% B lymphocytes, while about 60% of the cells are T lymphocytes (data not shown). Exposing the CBMCs to EBV leads to a marked expansion of the B lymphocytes by about 28 days after injection (Figure 2A). Analysis of human T cells in the spleen revealed significantly higher proportions of $CD8^+$ T cells in EBV-infected mice compared with noninfected controls (Figure 2B), suggesting that cytotoxic T lymphocytes (CTLs) are expanded in response to the viral infection. Moreover, histological analyses revealed that in addition to containing B lymphocytes, the tumors in these mice are also highly infiltrated by $CD8^+$ and $CD4^+$ T cells (Figure 2C). However, as we showed in a previous publication (35), the tumor B cells express inhibitory ligands such as PD-L1 and PD-L2 (Figure 2D), and this results in the autologous T cells being held in check. Consistent with the

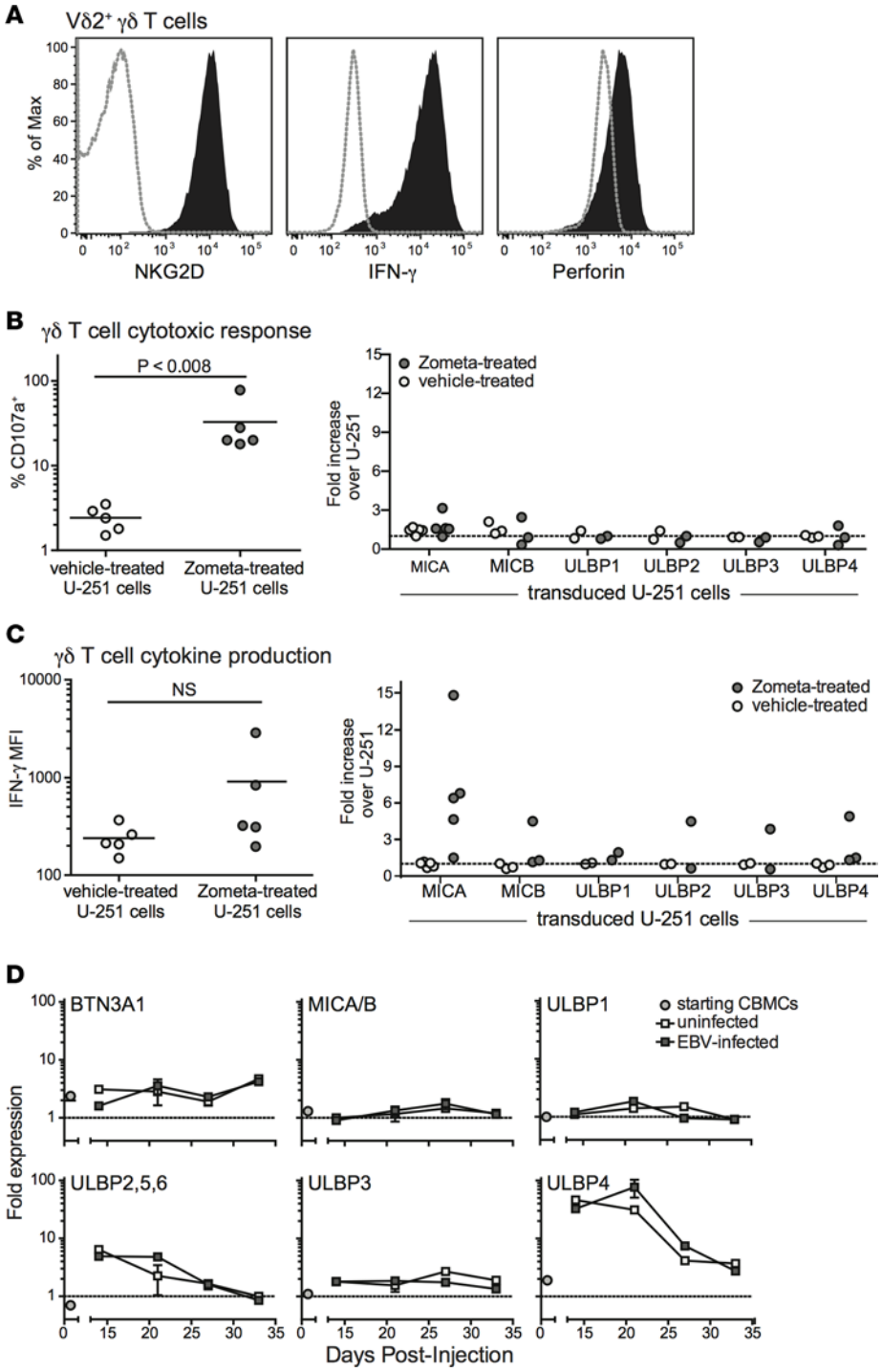

Figure 3. Analysis of TCR- and NKG2D-mediated Vδ2⁺ T cell responses. Vδ2⁺ T cells were expanded in vitro from adult human peripheral blood mononuclear cells by exposure to zoledronic acid (Zometa). (**A**) Flow cytometric analysis of the Vδ2⁺ T cells for cell surface expression of NKG2D, intracellular IFN-γ, and intracellular perforin (filled histograms). Dotted lines show staining with isotype-matched negative control mAbs. (**B**) The γδ T cell cultures were exposed for 4 hours to U-251 glioblastoma cells that were pretreated with Zometa to induce accumulation of isopentenylpyrophosphate, or mock-treated, and Vδ2⁺ T cell surface CD107a expression was assessed by flow cytometry. Left plot shows aggregated results from 5 independent experiments comparing the percentage of CD107a-positive cells in response to parental U-251 cells that express BTN3A1 but have little or no expression of NKG2D ligands. Right plot shows γδ T cell responses to U-251 transductants expressing the indicated NKG2D ligands; the percentage of CD107a⁺ Vδ2⁺ T cells responding to each transductant was normalized by the response to the parental U-251 cells. (**C**) Intracellular IFN-γ staining results from the experiments described in **B**. (**D**) Flow cytometric analysis was performed on uninfected human umbilical cord blood mononuclear cells (CBMCs) (circles), or on splenic B cells taken from mice given uninfected or EBV-treated CBMCs (light or dark gray squares, respectively) at the indicated times after injection. The cell surface expression of the indicated ligands is given as the median fluorescence intensity (MFI) obtained with the relevant specific mAb normalized by that from an isotype-matched negative control. Data points represent the mean values obtained from 1–4 separate analyses. NS, not significant.

presence of an inhibitory environment, we observed that T cells from tumor-bearing mice typically show less expression of the CD69 activation marker than their counterparts from mice engrafted with noninfected CBMCs (Figure 2E). Thus, this experimental model recapitulates an important hallmark of many cancers: endogenous T cells are present, but they are held in a suppressed state.

Characteristics of γδ T cells used for immunotherapy. Vγ9Vδ2⁺ T cells were expanded by culturing peripheral blood mononuclear cell (PBMC) samples from healthy adults in medium containing 2.5 μM zoledronic acid (Zometa) and 200 U/ml recombinant human IL-2 for 7–14 days, as previously described (36). Aminobisphosphonate drugs such as Zometa stimulate Vδ2⁺ T cell proliferation in a dose-dependent manner, because they block the mevalonate biosynthesis pathway and cause the accumulation of IPP, which then associates with BTN3A1 and is recognized by the TCR (11, 12). After this treatment, the PBMC cultures typically consisted of 80%–90% γδ T cells (Supplemental Figure 1; supplemental material available online with this article; https://doi.org/10.1172/jci.insight.93179DS1). Flow cytometric analysis confirmed that the expanded γδ T cells express the innate receptor NKG2D, and produce both IFN-γ and the cytolytic protein perforin (Figure 3A).

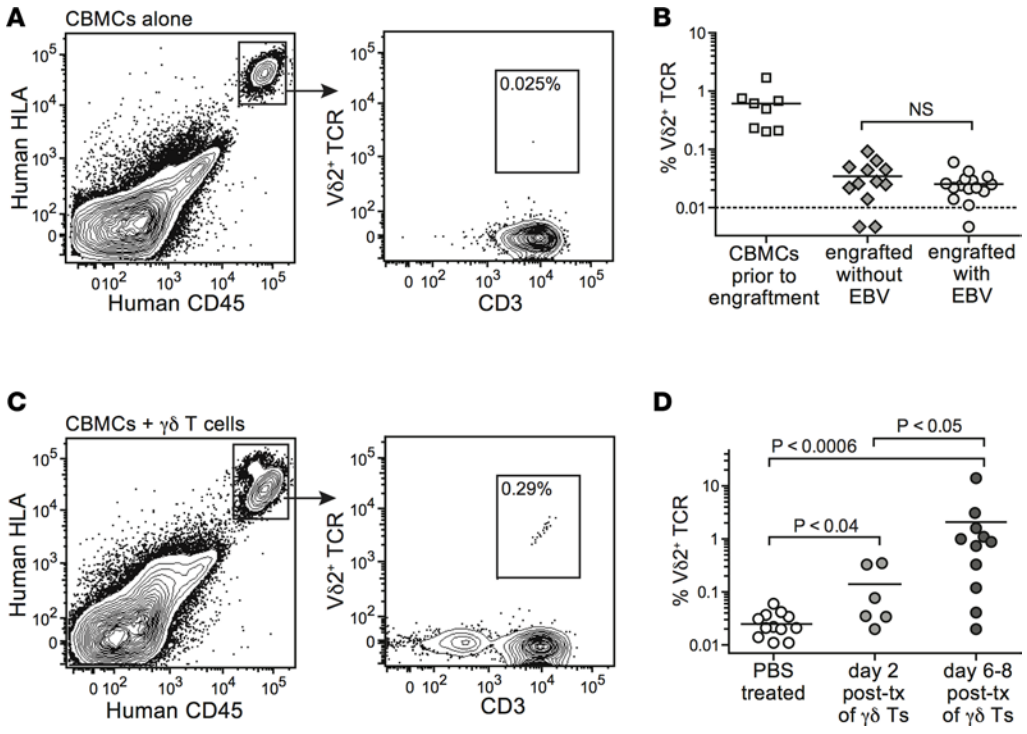

Figure 4. Vδ2⁺ T cells from engrafted cord blood do not expand in vivo in response to EBV infection, but adoptively transferred Vδ2⁺ T cells persist for at least 1 week. (**A**) Flow cytometric staining for human Vδ2⁺ T cells in the spleen of a representative mouse engrafted with human umbilical cord blood mononuclear cells (CBMCs) alone. (**B**) Aggregated results showing the percentage of T cells expressing a Vδ2⁺ TCR in starting CBMC samples compared with the percentage detected in spleens of CBMC-engrafted mice in the presence or absence of EBV infection. (**C**) Flow cytometric staining for human Vδ2⁺ T cells in the spleen of a representative CBMC-engrafted mouse that received adoptively transferred γδ T cells. (**D**) Aggregated results showing the percentage of Vδ2⁺ T cells in spleens of CBMC-engrafted mice given PBS (mock treatment) or in vitro–expanded γδ T cells. Spleens were harvested at the indicated times following administration of PBS or γδ T cells. *P* values were calculated using a 2-tailed nonparametric *t* test (Mann-Whitney analysis). NS, not significant; tx, transfer.

Prior studies have indicated that Vδ2⁺ T cells can respond to target cells via both TCR- and NKG2D-dependent mechanisms (21–23, 37, 38). To investigate the role of TCR- and NKG2D-mediated recognition in activating cytotoxic and cytokine responses by our expanded γδ T cells, we used a human glioblastoma cell line called U-251 MG. This cell line expresses low, but detectable levels of BTN3A1 at the cell surface, lacks detectable MICA and MICB, and has only minimal surface expression of ULBP molecules (Supplemental Figure 2). The γδ T cells were incubated with U-251 cells that were pretreated with vehicle alone or with Zometa, and T cell surface expression of CD107a (an indicator of recent cytolytic activity) was assessed by flow cytometry. Exposure to U-251 cells that had been sensitized with Zometa efficiently stimulated CD107a expression by the γδ T cells, whereas exposure to vehicle-treated U-251 cells induced very little CD107a upregulation (Figure 3B). Since Zometa sensitization exclusively impacts TCR-mediated recognition, these results indicate that cytotoxic responses by the expanded γδ T cells are activated by TCR stimulation. Notably, exposing the γδ T cells to retrovirally transduced U-251 cell lines that express high levels of individual NKG2D ligands did not lead to increased CD107a expression (Figure 3B), suggesting that costimulation by NKG2D does not enhance their cytotoxic responses. In contrast, a parallel analysis of IFN-γ production by the expanded γδ T cells suggested that target cell expression of NKG2D ligands can markedly costimulate cytokine production (Figure 3C).

To gain further insight, we assessed B cell expression of TCR and NKG2D ligands in our model system. The BTN3A1 glycoprotein was detectable on B cells in the CBMC samples used for engraftment, and its expression was maintained at similar levels following injection into NSG mice, regardless of whether the cells were exposed to EBV or not (Figure 3D). B cells in the starting CBMC sample showed little or no expression of NKG2D ligands (MICA/B, or ULBP1–6), and MICA/B molecules did not appear to become significantly upregulated after injection into the mice (Figure 3D). While 2 ULBP isoforms (ULBP2,5,6 and ULBP4) did show marked upregulation after transfer, this was not specific to the EBV-exposed cells. These results suggested that TCR-mediated pathways are available for activating γδ T cells in this model, but that NKG2D-mediated pathways are limited.

Detection of γδ T cells in vivo. The T cell compartment of human CBMC samples typically contains about 0.5%–2% Vδ2⁺ T cells (39). We investigated the frequencies of Vδ2⁺ cells within the human T cell compartment in spleens of mice engrafted with EBV-infected or uninfected CBMCs. Human cells in the murine spleens were readily delineated using mAbs specific for human HLA class I and human CD45 (Figure 4A). Analyses of splenocytes harvested 2–4 weeks after CBMC engraftment revealed only very low, or in some

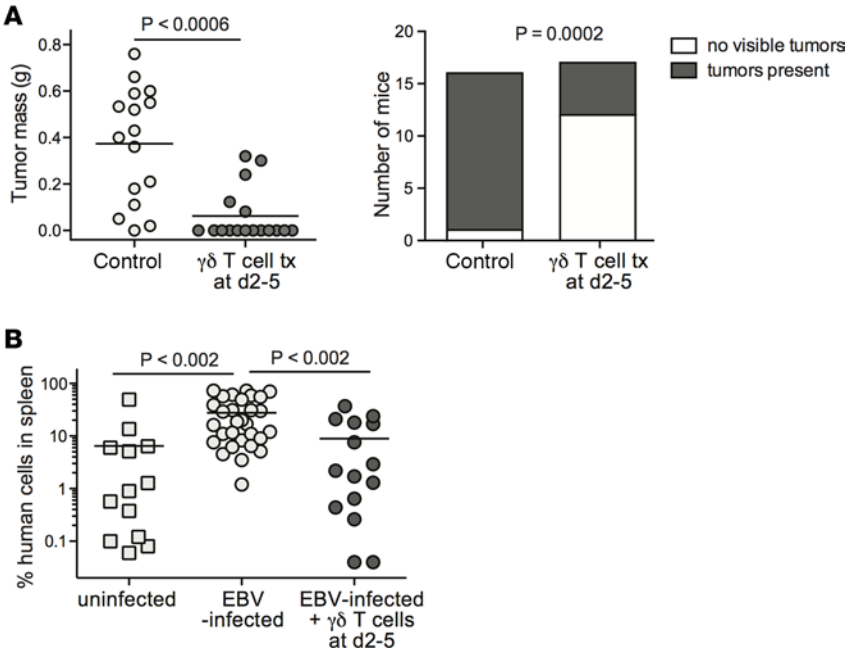

Figure 5. Early γδ T cell immunotherapy prevents tumor outgrowth and EBV-driven expansion of human cells in spleen. NSG mice were injected intraperitoneally with 10×10^6 EBV-treated human umbilical cord blood mononuclear cells (CBMCs). After 2–5 days, the mice were intravenously injected with a single dose of 5×10^6 to 10×10^6 γδ T cells, or not treated (control). Tumor and spleen tissues were harvested between 28 and 35 days after injection of the EBV-treated CBMCs, depending on when the control mice from the experiment appeared moribund. (**A**) Plots showing aggregated results from 3 independent experiments. Left plot shows tumor masses with each data point representing an individual mouse; the *P* value was calculated using a stratified nonparametric 2-tailed test (van Elteren analysis). Right plot shows the number of mice in each treatment group that had macroscopically visible tumor tissue, regardless of tumor mass; the *P* value was calculated using a 2-sided Fisher's exact *t* test. (**B**) Aggregated results from flow cytometric analysis showing the frequency of human cells in spleens of mice given mock-treated CBMCs (uninfected), or EBV-treated CBMCs with no immunotherapy (EBV-infected), or EBV-treated CBMCs followed by γδ T cells 2–5 days later. Each data point represents the result from an individual mouse. *P* values were calculated using a 2-tailed nonparametric *t* test (Mann-Whitney analysis). tx, transfer.

cases undetectable, frequencies of Vδ2$^+$ T cells (Figure 4, A and B). EBV infection did not result in increased Vδ2$^+$ T cell frequencies (Figure 4B). In contrast, flow cytometric analyses of CBMC-engrafted mice that were adoptively transferred with 1×10^6 to 5×10^6 in vitro–expanded γδ T cells consistently revealed a small but readily detectable population in the spleen (Figure 4C). Human Vδ2$^+$ T cells were detectable in spleens for at least 1 week after adoptive transfer, and their frequency appeared to increase somewhat during this time (Figure 4D), suggesting that they were not being rapidly eliminated by T cells derived from the CBMC sample.

Effects of γδ T cell immunotherapy. We investigated the impact of adoptive transfer of in vitro–expanded γδ T cells on the size and incidence of EBV-induced tumors. NSG mice were injected with EBV-exposed CBMCs and then given a single dose of γδ T cells 2–5 days later. This treatment had a significant impact on tumor outgrowth ($P < 0.0006$), with the majority of the γδ T cell–treated mice failing to develop macroscopically detectable tumors (Figure 5A). We also observed that the EBV-associated expansion of human cells in the spleen did not occur in mice that received γδ T cells within 1 week (Figure 5B), indicating that the effects of the γδ T cells are not limited to peritoneal sites of tumorigenesis. Thus, early time point γδ T cell therapy had effects that appeared consistent with immunosurveillance.

We next investigated the impact of administering γδ T cell therapy at later time points, after neoplastic changes to lymphoid masses in the peritoneal cavity are typically apparent. NSG mice were injected with EBV-exposed CBMCs, and injected with a single dose of γδ T cells or vehicle (sterile PBS) 22–25 days later. The mice were sacrificed 5–7 days after administration of the immunotherapy, and peritoneal tissue was collected for analysis. Compared with the vehicle-treated mice, those that received γδ T cells showed significantly reduced peritoneal tumor mass ($P < 0.00002$) (Figure 6A). Notably, this single-dose, late time point immunotherapy protocol did not usually result in a complete eradication of tumor tissue (Figure 6B).

PD-1 expression of adoptively transferred γδ T cells. We have recently shown that the administration of checkpoint-blockade antibodies (anti–PD-1 and anti-CTLA4) results in reduced tumor burden and enhanced survival in this model (35). Together with additional findings (e.g., that checkpoint inhibition was associated with improved EBV antigen–specific IFN-γ secretion by T cells from EBV-infected mice), these results suggested that antitumor T cell responses are usually held in check by inhibitory ligands in this model. Based on these prior observations, we were surprised at the dramatic antitumor effects of γδ T cells that were administered without additional measures to provide checkpoint blockade. However, flow cytometric analysis of splenic T cells from adoptively transferred mice revealed that the γδ T cell subset showed very low PD-1 expression compared with CD8$^+$ T cells and most of the CD4$^+$ T cells (Figure 7A). Thus, low PD-1 expression might be key to the antitumor efficacy of immunotherapeutic γδ T cells, but the stability of this state was not clear.

To further investigate, we assessed PD-1 expression by γδ T cells in adult human PBMC samples directly ex vivo, and at a series of time points during our in vitro expansion protocol. There was little cell surface

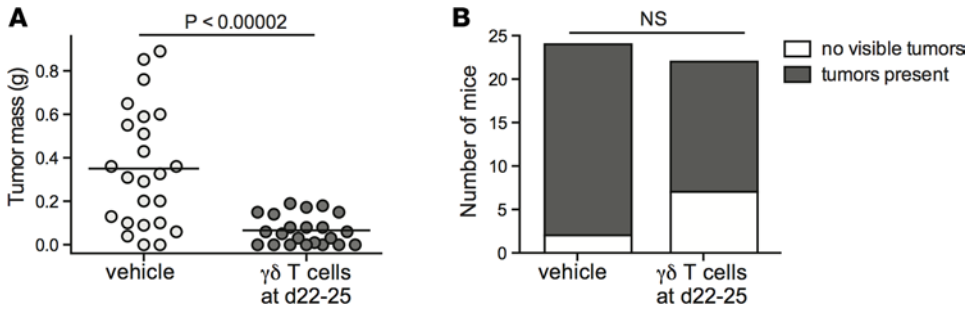

Figure 6. Administration of γδ T cell immunotherapy after onset of neoplastic transformation limits tumor size. NSG mice were injected intraperitoneally with 10×10^6 EBV-treated human umbilical cord blood mononuclear cells (CBMCs). After 22–25 days, the mice were intravenously injected with a single dose of 5×10^6 to 10×10^6 γδ T cells or sterile PBS (vehicle). (**A**) Plot showing aggregated results of tumor mass from 4 independent experiments, with each data point representing an individual mouse; the *P* value was calculated using a stratified nonparametric 2-tailed test (van Elteren analysis). (**B**) Plot showing the number of mice in each treatment group that had macroscopically visible tumor tissue, regardless of tumor mass. NS, not significant based on a 2-sided Fisher's exact *t* test.

PD-1 on Vδ2$^+$ T cells in the starting PBMC samples, but the expression of this ligand was markedly upregulated over the first 4 days of exposure to Zometa in vitro (Figure 7B). However, thereafter the PD-1 expression levels dropped, and by 7 days of in vitro expansion (the time at which the γδ T cell frequency in the culture typically reaches its maximum) the PD-1 expression had returned nearly to baseline (Figure 7B).

We next tested the impact of adoptive transfer into CBMC-engrafted mice on the expression of PD-1 by in vitro–expanded γδ T cells. A PBMC sample that stained positively for HLA-A2 was cultured with Zometa for varying lengths of time, and then 5×10^6 cultured cells per mouse were injected intravenously into NSG mice that had been engrafted 3 weeks earlier with an HLA-A2–negative CBMC sample. Five days after the adoptive transfer, splenocytes were harvested and PD-1 expression levels were assessed on HLA-A2$^+$ γδ T cells. As shown in Figure 7C, PD-1 expression levels on the splenic γδ T cells after 5 days in vivo closely matched the PD-1 expression levels present on the γδ T cells at the time they were injected. Thus, the initial level of PD-1 expression on adoptively transferred γδ T cells appeared to be maintained in vivo.

Finally, we performed an experiment to compare PD-1 expression by adoptively transferred γδ versus αβ T cells. A PBMC sample that stained positively for HLA-A2 was expanded for 8 days with a slightly suboptimal concentration of Zometa, resulting in a mixed culture of 67% γδ and 33% αβ T cells. These cells were injected into EBV-infected mice engrafted with HLA-A2–negative CBMCs. CBMC-derived and adoptively transferred T cells in the spleens of the mice were analyzed by flow cytometry for PD-1 expression levels (Figure 7D). The adoptively transferred γδ T cells consistently showed lower PD-1 expression than the transferred αβ T cells, while the CBMC-derived T cells showed very high PD-1 expression (Figure 7E). Together, these results underscore the selectivity of low PD-1 expression by our immunotherapeutic γδ T cells.

Analysis of tumors after late γδ T cell treatment. Histological analyses of tissue slides from γδ T cell–treated mice frequently showed CD3$^+$ cells that localized to areas of the tumors containing high frequencies of cells expressing the EBV protein EBNA2 (Figure 8A). Interestingly, however, careful inspection of tumor sections often revealed the presence of CD3$^+$ cells in the lumens of blood vessels within the tumors (Figure 8A), suggesting active trafficking of T cells. Flow cytometric analyses of the frequency of γδ T cells found in spleen and tumor tissues from the same mice suggested there was a trend towards increased γδ T cell representation in tumors compared with spleens (Figure 8B). Moreover, using HLA-A2 expression to specifically track the adoptively transferred population, we observed that at 2 days after injection of a mixed population of αβ and γδ T cells (67% γδ, 33% αβ), the transferred γδ T cells appeared significantly more enriched in the tumor tissue than the transferred αβ T cells. In contrast, in the spleen the proportion of adoptively transferred γδ versus αβ T cells was close to that of the initial mixture (Figure 8B).

Further flow cytometric analysis revealed that mice that received late time point γδ T cell immunotherapy had B cell frequencies similar to those of mock-treated mice at 2–3 days after transfer, but by 5–8 days after transfer there was a significant reduction in B cell frequency in tumors of γδ T cell–treated mice (Figure 8C). Additionally, the γδ T cell therapy appeared to be associated with reduced surface expression of PD-L1 and PD-L2 on tumor B cells, compared with those from vehicle-treated mice (Figure 8D). Together, these results suggested that although the adoptively transferred γδ T cells localized to both spleen and tumor

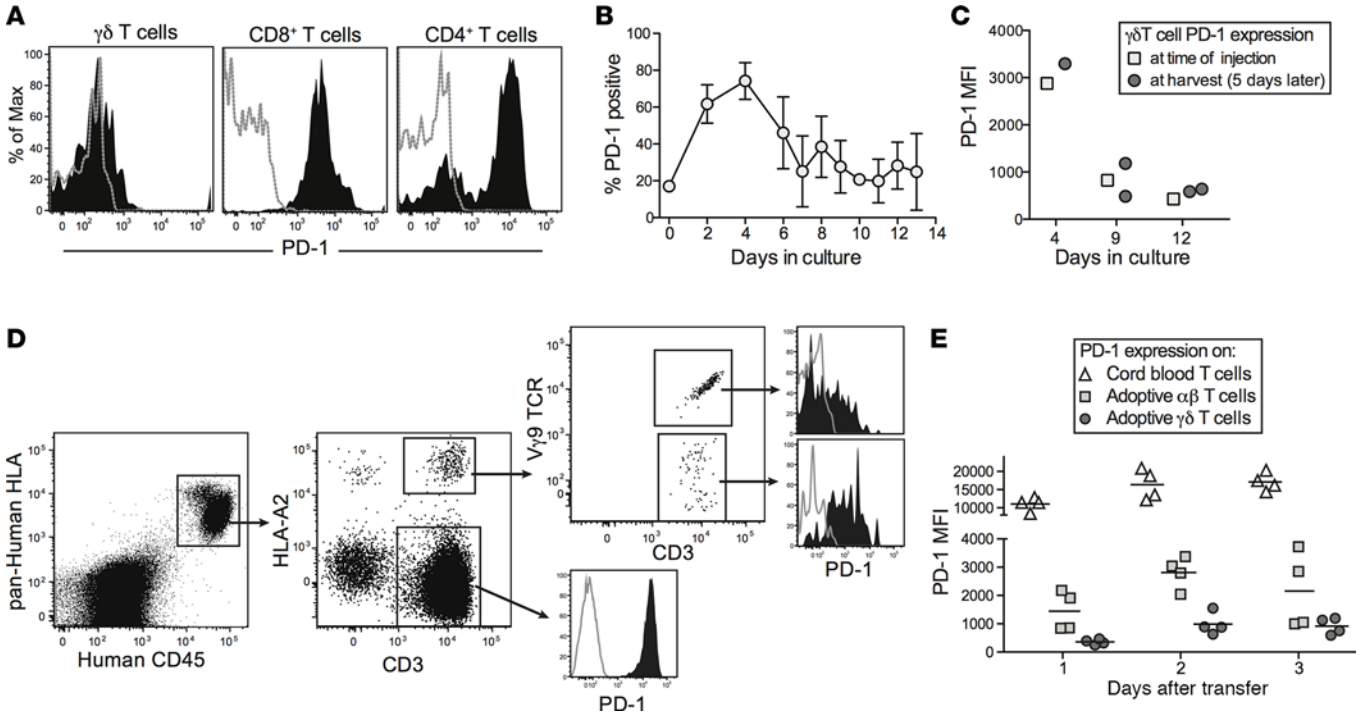

Figure 7. Low PD-1 expression maintained in vivo by adoptively transferred γδ T cells. (**A**) Analysis of PD-1 expression by human T cell subsets from an EBV-infected mouse that was administered γδ T cells that had been expanded in vitro for 8 days. Filled histograms show anti–PD-1 staining; gray dotted lines show staining by an isotype-matched control mAb. (**B**) Expression of PD-1 by Vδ2⁺ T cells over the course of in vitro expansion. Total human peripheral blood mononuclear cells freshly isolated from healthy adult donors were cultured in medium containing 2.5 μM zoledronic acid (Zometa), and expression of PD-1 on Vδ2⁺ T cells was assessed by flow cytometry at the indicated time points. Data points show the means and standard deviations of results from 3–5 independent experiments taken at the indicated time points. (**C**) Plot showing PD-1 expression by in vitro–expanded γδ T cells immediately prior to injection into human umbilical cord blood mononuclear cell–engrafted (CBMC-engrafted) NSG mice (squares) or at the time of harvest from spleens 5 days later (circles). Adoptively transferred γδ T cells were differentiated from the CBMCs used for engraftment by analysis of HLA-A2 expression, which was intentionally mismatched. (**D**) EBV-infected mice were administered a mixed population of αβ and γδ T cells (approximately 35% αβ and 65% γδ) obtained by culture with a suboptimal concentration of Zometa. Flow cytometric analysis of splenocytes showing PD-1 expression by the adoptively transferred T cells (HLA-A2 positive) segregated according to γδ TCR expression, compared with T cells from the CBMC sample that was used for the initial engraftment (HLA-A2 negative). (**E**) Plot showing PD-1 expression by the indicated splenic T cell populations from 4 separate mice.

tissue, in the first 2 days after injection the γδ T cells may tend to preferentially accumulate within tumors. At somewhat later time points (5–7 days after injection), γδ T cell therapy was associated with changes to the frequency and PD-L1/L2 phenotype of B cells in residual tumors.

Discussion

It is now clear that suppressive effects mediated by the upregulation of inhibitory B7 family members within tumor microenvironments are an important factor in the failure of cytolytic lymphocytes to control tumors (40, 41). A central issue for cellular immunotherapies is therefore avoiding inhibition of adoptively transferred cells by these pathways. We have recently shown that in our in vivo model of EBV-driven B lymphomagenesis, the antitumor effects of endogenous human T cells are limited by checkpoint inhibition mediated via PD-1 and CTLA-4 (35). Here, we show that adoptively transferred Vδ2⁺ T cells expanded from human PBMCs have potent antitumor effects, even without coadministering checkpoint inhibitors. Remarkably, after completing their most active phase of Zometa-induced expansion in vitro, the γδ T cells we used for immunotherapy show only low levels of PD-1 expression, and their PD-1^{lo} status is maintained after transfer into CBMC-engrafted NSG mice. These findings suggest an intriguing rationale for why the immunotherapeutic γδ T cells are able to mediate strong antitumor effects: they are likely less affected than the endogenous T cells by inhibitory ligands expressed by the tumor B cells. Thus, in addition to supporting the potential clinical utility of in vitro–expanded Vδ2⁺ T cells, our analysis suggests that a key area for future investigation will be to understand in detail the regulation of PD-1 expression on human γδ T cells that are to be used for cellular immunotherapy.

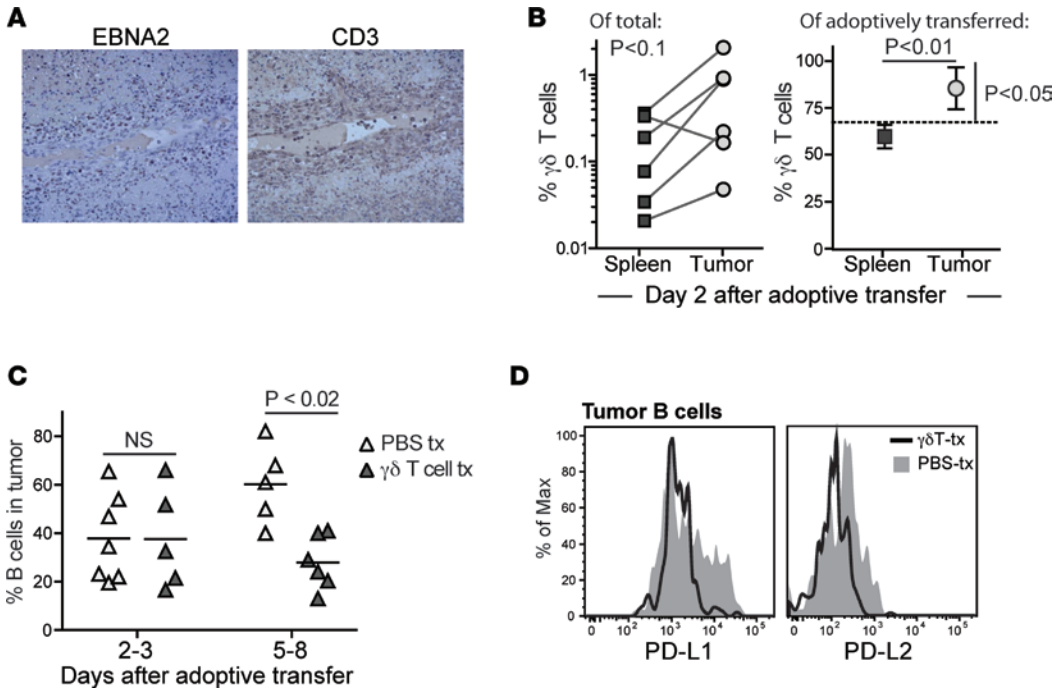

Figure 8. Recruitment of γδ T cells and analysis of tumor B cells after late time point γδ T cell administration. (**A**) Light microscopic images (×10 magnification) of IHC of serial sections of tumor tissue from a γδ T cell–treated mouse showing cells expressing the viral protein EBNA2 (left image) or CD3 (right image). T cells are observed within the blood vessel in the middle of the field, as well as infiltrating the surrounding tissue in areas where EBNA2$^+$ cells are localized. (**B**) Adoptively transferred γδ T cells appear slightly enriched in tumor tissue compared with spleen. Left plot: percentage of human T cells expressing Vδ2 in paired spleen versus tumor tissue samples from independent mice. Tissues were harvested 2 days after administration of γδ T cell immunotherapy. The *P* value was calculated using a paired, nonparametric *t* test (Wilcoxon signed-rank test). Right plot: percentage of the adoptively transferred cells in spleen versus tumor expressing a Vγ2Vδ2$^+$ TCR. The dashed line shows the frequency of γδ T cells in the injected population; symbols show mean and standard deviations of 4 replicate analyses each of spleen and tumor tissue. The *P* value comparing spleen versus tumor frequencies (horizontal line) was calculated using an unpaired parametric *t* test; the *P* value comparing tumor mean to the γδ T cell frequency of the injected cells (vertical bar) was calculated using a 1-sample, 2-tailed *t* test. (**C**) B cells as a percentage of the total human cells in tumor tissue from a series of mice that were administered γδ T cells (dark triangles) or vehicle (light triangles). Tumors were harvested at the indicated times after adoptive transfer or mock treatment. The *P* value was calculated using a 2-tailed nonparametric *t* test (Mann-Whitney analysis). (**D**) Flow cytometric analysis of PD-L1 and PD-L2 staining on tumor B cells. Filled gray histograms show results from a mouse given vehicle (PBS-tx); black line shows results from a mouse given γδ T cells. tx, transfer.

A study by Xiang et al. recently established that similar in vitro–expanded human Vδ2$^+$ T cells can control the growth in vivo of human B lymphoblastoid cell lines that were first transformed by EBV in vitro and then transferred into NSG mice (32). While providing a powerful demonstration that high doses of Vδ2$^+$ T cells are sufficient to kill EBV-transformed B lymphoblastoid cells in vivo, the analysis by Xiang et al. did not address the more physiological scenario that we have created in our model, where we have tested the antitumor impact of a comparatively small number of adoptively transferred γδ T cells in the presence of a much larger number of autologous T cells that are functionally suppressed. Additionally, by performing our studies with a strain of EBV (M81) that produces a mixture of lytic and latent infection (42), rather than the B95-8 laboratory strain that establish mainly latent infection, we have created a more physiologically relevant model where the nature of the viral infection may vary in different anatomical locations. For example, while expression of lytic EBV proteins appears diminished in the spleen compared with tumors (Figure 1E), we have observed dispersed positive staining in the spleen for viral latency proteins such as EBNA1 (data not shown), suggesting that EBV-infected cells in that location may be in a less active state of infection. Interestingly, we have found that in contrast to the effect on tumors, administration of γδ T cells at late time points does not seem to result in reduced frequencies of B cells in the spleen (Supplemental Figure 3). Thus, it appears that the adoptively transferred γδ T cells do not target splenic B cells in this model, despite the presence of latent EBV infection at that location.

It is not clear how the immunotherapeutic Vδ2$^+$ T cells might distinguish between B cells in spleen versus tumor in this model. One mechanism that might explain this is that the tumor B cells may overproduce cellular prenylpyrophosphate compounds (e.g., IPP) that activate Vδ2$^+$ T cells, perhaps as a result of their

more aggressive viral gene expression, compared with EBV-infected B cells in the spleen. This mechanism would be consistent with the observations from our in vitro analyses using U-251 cells (Figure 3B), which suggested that IPP accumulation provides the major signal to activate the cytolytic responses of our immunotherapeutic Vδ2$^+$ T cells. However, we have not determined whether the in vivo antitumor effects of the Vδ2$^+$ T cells involve TCR-mediated recognition, or whether other ligands may be involved that distinguish the tumor B cells from those in the spleen. Similarly, it is not clear whether the effects of the immunotherapeutic γδ T cells in this model are due to direct cytolysis of tumor cells, or to a different mechanism such as cytokine secretion, or even by serving as highly stimulatory antigen-presenting cells (APCs) for HLA-restricted T cells, as reported previously by others (43–46).

Another important caveat to our study is the presence of a contaminating fraction of αβ T cells (typically less than 20%) within the Zometa-expanded T cell cultures that we used for immunotherapies. Our results suggest that these contaminating T cells do not mediate strong effector functions in vivo since they appear not to localize efficiently to the tumor tissue and they show more elevated PD-1 expression (Figures 7 and 8). Additionally, since they are allogeneic to the B cells in this model they might be expected to target those in the spleen as well as the tumors, which we do not observe (Supplemental Figure 3). To confirm the lack of effector responses by conventional T cells, we tested whether we could detect EBV peptide–specific T cell responses from mice that had received the immunotherapeutic cell mixture. As shown in Supplemental Figure 4, we did not observe responses to EBV peptides by T cells harvested from mice that received adoptive therapy, although we did detect a response to anti-CD3 stimulation. Nevertheless, removal of these contaminating T cells is likely to be an important consideration before translation to clinical scenarios.

Phase I clinical trials involving adoptively transferred γδ T cells carried out thus far have yielded somewhat mixed results. Four trials have shown results consistent with an antitumor effect of the therapy. Two were trials involving patients who had advanced renal cell carcinomas; in one, 3 out of 5 patients who received adoptive transfer of aminobisphosphonate-expanded γδ T cells showed delayed tumor doubling time (47), and in the other (a phase I/II trial) all 11 patients who received Zometa-expanded γδ T cells and recombinant IL-2 showed prolonged tumor doubling time (48). In another trial involving 18 subjects with metastatic solid tumors who received adoptive transfer of Zometa-expanded γδ T cells in combination with Zometa and IL-2, three patients showed measurable disease responses (49). Finally, in a trial of 4 patients with advanced hematological malignancies who received haploidentical transplants highly enriched for γδ T cells followed by in vivo administration of Zometa and IL-2, three subjects showed complete remission lasting more than 6 months while one died of an infection 6 weeks after the cell transfusion (50).

In contrast, several other phase I trials, while providing data that γδ T cell adoptive therapy is well tolerated, have not shown clear evidence of antitumor effects. In a trial involving 6 subjects with multiple myeloma who received Zometa-expanded γδ T cells in combination with Zometa and IL-2, four of the subjects showed M protein levels that remained at baseline, but there was no clear correlation between the amount of γδ T cells infused and clinical outcomes (51). In a study of 10 patients with metastatic renal cell carcinoma who received γδ T cells expanded using bromohydrin pyrophosphate and IL-2, six subjects showed stabilized disease but there was no clear antitumor effect (52). Finally, in 2 studies of non–small cell lung cancer involving 10 and 15 patients, respectively, who received Zometa-expanded γδ T cells and IL-2, there were no objective indicators of success although about one-third to one-half of the patients showed stable disease after therapy (53, 54).

What is clear from these published clinical trials is that in addition to variation in the types of cancer treated, there is little consistency in the protocols used to expand γδ T cells in vitro for cellular immunotherapy, or in how the immunotherapy was delivered (e.g., γδ T cells alone, or in combination with activating agents such as IL-2 and Zometa). Our results suggest that in addition to standardizing these factors, it will be important to evaluate PD-1 expression of immunotherapeutic γδ T cells expanded in vitro. Our preclinical model of B lymphomagenesis is thus likely to be highly useful for studies aimed at understanding how to optimize the antitumor effects of human Vδ2$^+$ T cells as agents of cellular immunotherapy, as well as further delineating their activation requirements and mechanisms of action in vivo.

Methods

Preparation of EBV. All experiments were performed using the lytic M81 strain of EBV. M81 bacmid expressing green fluorescent protein (GFP) and a hygromycin B resistance gene was constructed using bacterial artificial chromosome technology as described (42). Infectious viral particles were produced from

293 cell lines that were stably infected with the M81 strain of EBV following transfection with EBV BZLF1 expression vector as previously described (55). The titer of infectious EBV was determined by assessing the number of fluorescent Raji cells derived from serial dilutions of the concentrated virus stock and calculating the green Raji unit (GRU) titer, as previously described (55).

In vivo model. Human umbilical CBMCs were purified by density gradient centrifugation using Ficoll Paque PLUS (GE Healthcare), washed in sterile PBS, followed by 2 low-speed centrifugation spins (200–300 *g*) to remove platelets, and if necessary to diminish red blood cell contamination they were treated briefly with ammonium-chloride-potassium (ACK) lysis buffer. The CBMCs were then suspended in tissue culture medium (RPMI 1640 with L-glutamine [Corning] and supplemented with 10% bovine calf serum [Thermo Fisher Scientific], 3% human AB serum [Atlanta Biologicals], 1% penicillin/streptomycin [Mediatech]) and exposed to 2,000 U of the M81 strain of EBV, or mock treated in medium alone, for 2 hours. Finally, the CBMCs were washed and resuspended in sterile PBS, and 10×10^6 cells per mouse were injected intraperitoneally into 6- to 8-week-old NOD.Cg-Prkdc^{scid}Il2rg^{tm1Wjl}/SzJ (NSG) mice (Jackson Labs). Mice were maintained in a specific pathogen–free facility using sterilized cages, bedding, food, and water, and were euthanized at day 29–30 or when they appeared moribund on the basis of weight loss and body condition score. Grossly visible tumor tissue was carefully excised and weighed, and tissues were harvested for further analysis.

Expansion of Vδ2$^+$ T cells from PBMCs and adoptive transfer into mice. PBMCs were isolated from venous blood samples from healthy donors obtained in accordance with a protocol approved by the University of Wisconsin Minimal Risk IRB. Written informed consent for experimental use of cells was obtained from all donors. Blood was processed by density gradient centrifugation using Ficoll-paque PLUS according to the manufacturer's protocol. To expand Vδ2$^+$ T cells, freshly isolated PBMCs were exposed for 7–14 days to 2.5 μM Zometa (Novartis) and 200 units/ml IL-2, in tissue culture medium that was composed of RPMI 1640 containing L-glutamine, 15% heat-inactivated bovine calf serum (Thermo Fisher Scientific), 3% human AB serum, and 100 μg/ml each of penicillin and streptomycin. The expanded Vδ2$^+$ T cells were washed and resuspended in sterile PBS, then administered intravenously via retro-orbital injection to anesthetized mice at the indicated day. For immunotherapy treatment studies, 5×10^6 to 10×10^6 Vδ2$^+$ T cells per mouse were injected; for tumor infiltration studies, 1×10^6 to 5×10^6 Vδ2$^+$ T cells per mouse were injected.

Generation and analysis of U-251 cells expressing NKG2D ligands. U-251 MG cells (formerly known as U-373 MG cells) stably expressing the NKG2D ligands ULBP1, ULBP2, ULBP3, ULBP4, MICA, or MICB were generated by retroviral transduction using the vector pLNCX (Clontech), as previously described (56). The U-251 parental cells and retroviral transductants were incubated overnight in culture medium (DMEM supplemented with 5% heat-inactivated bovine calf serum, 5% fetal bovine serum, and 100 μg/ml each of penicillin and streptomycin) in the presence or absence of 1.25 μM Zometa. The U-245 cells were washed and combined at a 1:1 ratio with Vδ2$^+$ T cells expanded from PBMCs. After a 6-hour coincubation, the cells were harvested, washed, and Fc receptors were blocked by incubation in PBS containing 20% human AB serum. Cells were stained with antibodies against CD3, Vδ2 TCR, and CD107a (BioLegend; clone OKT3, B6, and H4A3, respectively) or an isotype-matched control monoclonal antibody. Where indicated, intracellular cytokine staining for IFN-γ (BioLegend; clone 4S.B3) was also performed using the BD Cytofix/Cytoperm kit (BD Biosciences).

Histological analyses. Tissues were fixed in 10% buffered formalin and embedded in paraffin prior to sectioning. Sections were deparaffinized and processed for H&E staining, immunohistochemistry, or in situ hybridization. Immunohistochemistry was performed using an antibody against the EBV protein EBNA1 (clone 1EB14, Santa Cruz Biotechnology Inc.), or with the following antibodies against human cellular antigens: CD20 (clone H1, BD-Pharmingen); CD4 (clone 4B12, Leica Microsystems); CD8 (clone SP16, Biocare Medical LLC). Antigen retrieval was performed using Rodent Decloaker (Biocare Medical). Antibody labeling was detected and visualized using a horseradish peroxidase (HRP)-polymer kit with diaminobenzidine (DAB) development (Biocare Medical). EBER detection was performed by in situ hybridization using the PNA ISH Detection Kit (DakoCytomation).

Flow cytometric analysis. Single-cell suspensions were pelleted, washed, and resuspended in PBS containing 15% human AB serum to block Fc receptors. Staining was performed using fluorescently labeled monoclonal antibodies specific for human cell surface markers, and compared to isotype-matched negative control antibodies used for fluorescence minus one (FMO) conditions. The following antibodies used for staining were purchased from BioLegend: anti–HLA-A,B,C (clone W6/32), anti-CD45 (clone HI30), anti-CD3 (clone OKT3), anti-CD4 (clone OKT4), anti-CD8 (clone RPA-T8), anti-CD19 (clone HIB19),

anti-CD20 (clone 2H7), anti–PD-L1 (clone 29E.2A3), anti–PD-L2 (clone 24F.10C12), anti–PD-1 (clone EH12.2H7), anti-CD69 (clone FN50), anti-NKG2D (clone 1D11), anti-BTN3A1 (clone BT3.1), anti-MICA/B (clone 6D4), and anti-Vδ2 (clone B6). Additionally, the following monoclonal antibodies were purchased from R&D Systems: anti-ULBP1 (clone 170818), anti-ULBP2/5/6 (clone 165903), anti-ULBP3 (clone 166510), and anti-ULBP4 (clone 709116). Compensation was performed using single-color controls, and staining was detected using an LSRII flow cytometer (BD Biosciences). Flow cytometric data were analyzed using FlowJo software v9.3.1 (Tree Star).

Statistics. Experimental datasets that consisted of independent analyses of individual mice were analyzed using a 2-tailed, nonparametric *t* test (Mann-Whitney analysis); datasets that consisted of replicate analyses of samples from the same mouse were analyzed using an unpaired, 2-tailed parametric *t* test. For datasets where treatment groups from independent experiments were aggregated, statistical analysis was performed using the van Elteren test to account for the effect of stratification. *P* values of 0.05 or less were considered significant.

Study approval. Experimental protocols involving animals were approved by the University of Wisconsin-Madison IACUC, and work involving animals was conducted in accordance with the NIH Guide for the care and use of laboratory animals. Deidentified human umbilical CBMCs were obtained from the University of Colorado Cord Blood Bank, and analyzed according to an IRB protocol approved by the University of Wisconsin Minimal Risk IRB.

Author contributions

JEG designed the research studies, wrote the manuscript, and prepared figures. NAZ, AS, XX,and SM conducted experiments and acquired data. NAZ, AGF, and JEG analyzed and interpreted data. JRM, SCK, CLS, and AWH provided critical reagents.

Acknowledgments

Primary funding for this work was provided by a pilot grant from the University of Wisconsin Carbone Cancer Center that was supported in part by NIH grant NCI P30 CA014520. Additional funding was provided by the following NIH grants: R21 AI116007 to JEG; R21 AI105847 and R01 AI069099 to AWH; R01 CA174462 and P01-CA022443 to SCK; support from T32 CA157322 for NAZ. The funders had no role in study design, data collection and analysis, decision to publish, or preparation of the manuscript.

Address correspondence to: Jenny E. Gumperz, Department of Medical Microbiology and Immunology, University of Wisconsin School of Medicine and Public Health, Microbial Sciences Building, Room 4305, 1550 Linden Dr., Madison, Wisconsin 53706, USA. Phone: 608.263.6902; Email: jegumperz@wisc.edu.

SM's present address is: Sanofi, Inc., Cambridge, Massachusetts, USA.

CLS's present address is: Carroll University, Waukesha, Wisconsin, USA.

1. Moingeon P, et al. A unique T-cell receptor complex expressed on human fetal lymphocytes displaying natural-killer-like activity. *Nature*. 1986;323(6089):638–640.
2. Sturm E, Braakman E, Fisch P, Vreugdenhil RJ, Sondel P, Bolhuis RL. Human V gamma 9-V delta 2 T cell receptor-gamma delta lymphocytes show specificity to Daudi Burkitt's lymphoma cells. *J Immunol*. 1990;145(10):3202–3208.
3. Fisch P, et al. Gamma/delta T cell clones and natural killer cell clones mediate distinct patterns of non-major histocompatibility complex-restricted cytolysis. *J Exp Med*. 1990;171(5):1567–1579.
4. Ensslin AS, Formby B. Comparison of cytolytic and proliferative activities of human gamma delta and alpha beta T cells from peripheral blood against various human tumor cell lines. *J Natl Cancer Inst*. 1991;83(21):1564–1569.
5. Strid J, et al. Acute upregulation of an NKG2D ligand promotes rapid reorganization of a local immune compartment with pleiotropic effects on carcinogenesis. *Nat Immunol*. 2008;9(2):146–154.
6. Liu Z, Eltoum IE, Guo B, Beck BH, Cloud GA, Lopez RD. Protective immunosurveillance and therapeutic antitumor activity of gammadelta T cells demonstrated in a mouse model of prostate cancer. *J Immunol*. 2008;180(9):6044–6053.
7. Ma C, et al. Tumor-infiltrating γδ T lymphocytes predict clinical outcome in human breast cancer. *J Immunol*. 2012;189(10):5029–5036.
8. Coffelt SB, et al. IL-17-producing γδ T cells and neutrophils conspire to promote breast cancer metastasis. *Nature*. 2015;522(7556):345–348.
9. De Libero G. Tissue distribution, antigen specificity and effector functions of gamma delta T cells in human diseases. *Springer*

Semin Immunopathol. 2000;22(3):219–238.
10. Fisher JP, et al. Neuroblastoma killing properties of Vδ2 and Vδ2-negative γδT cells following expansion by artificial antigen-presenting cells. *Clin Cancer Res*. 2014;20(22):5720–5732.
11. Vavassori S, et al. Butyrophilin 3A1 binds phosphorylated antigens and stimulates human γδ T cells. *Nat Immunol*. 2013;14(9):908–916.
12. Wang H, et al. Butyrophilin 3A1 plays an essential role in prenyl pyrophosphate stimulation of human Vγ2Vδ2 T cells. *J Immunol*. 2013;191(3):1029–1042.
13. Sandstrom A, et al. The intracellular B30.2 domain of butyrophilin 3A1 binds phosphoantigens to mediate activation of human Vγ9Vδ2 T cells. *Immunity*. 2014;40(4):490–500.
14. Wang H, Morita CT. Sensor function for butyrophilin 3A1 in prenyl pyrophosphate stimulation of human Vγ2Vδ2 T cells. *J Immunol*. 2015;195(10):4583–4594.
15. Rhodes DA, et al. Activation of human γδ T cells by cytosolic interactions of BTN3A1 with soluble phosphoantigens and the cytoskeletal adaptor periplakin. *J Immunol*. 2015;194(5):2390–2398.
16. Riaño F, et al. Vγ9Vδ2 TCR-activation by phosphorylated antigens requires butyrophilin 3 A1 (BTN3A1) and additional genes on human chromosome 6. *Eur J Immunol*. 2014;44(9):2571–2576.
17. Tanaka Y, Morita CT, Tanaka Y, Nieves E, Brenner MB, Bloom BR. Natural and synthetic non-peptide antigens recognized by human gamma delta T cells. *Nature*. 1995;375(6527):155–158.
18. Gober HJ, Kistowska M, Angman L, Jenö P, Mori L, De Libero G. Human T cell receptor gammadelta cells recognize endogenous mevalonate metabolites in tumor cells. *J Exp Med*. 2003;197(2):163–168.
19. Champsaur M, Lanier LL. Effect of NKG2D ligand expression on host immune responses. *Immunol Rev*. 2010;235(1):267–285.
20. Lanier LL. NKG2D receptor and its ligands in host defense. *Cancer Immunol Res*. 2015;3(6):575–582.
21. Das H, et al. MICA engagement by human Vgamma2Vdelta2 T cells enhances their antigen-dependent effector function. *Immunity*. 2001;15(1):83–93.
22. Bauer S, et al. Activation of NK cells and T cells by NKG2D, a receptor for stress-inducible MICA. *Science*. 1999;285(5428):727–729.
23. Rincon-Orozco B, Kunzmann V, Wrobel P, Kabelitz D, Steinle A, Herrmann T. Activation of V gamma 9V delta 2 T cells by NKG2D. *J Immunol*. 2005;175(4):2144–2151.
24. Chitadze G, Bhat J, Lettau M, Janssen O, Kabelitz D. Generation of soluble NKG2D ligands: proteolytic cleavage, exosome secretion and functional implications. *Scand J Immunol*. 2013;78(2):120–129.
25. Pang DJ, Neves JF, Sumaria N, Pennington DJ. Understanding the complexity of γδ T-cell subsets in mouse and human. *Immunology*. 2012;136(3):283–290.
26. Afrache H, Gouret P, Ainouche S, Pontarotti P, Olive D. The butyrophilin (BTN) gene family: from milk fat to the regulation of the immune response. *Immunogenetics*. 2012;64(11):781–794.
27. Malkovska V, Cigel FK, Armstrong N, Storer BE, Hong R. Antilymphoma activity of human gamma delta T-cells in mice with severe combined immune deficiency. *Cancer Res*. 1992;52(20):5610–5616.
28. Chen J, Niu H, He W, Ba D. Antitumor activity of expanded human tumor-infiltrating gammadelta T lymphocytes. *Int Arch Allergy Immunol*. 2001;125(3):256–263.
29. Zheng BJ, et al. Anti-tumor effects of human peripheral gammadelta T cells in a mouse tumor model. *Int J Cancer*. 2001;92(3):421–425.
30. Lozupone F, et al. Effect of human natural killer and gammadelta T cells on the growth of human autologous melanoma xenografts in SCID mice. *Cancer Res*. 2004;64(1):378–385.
31. Kabelitz D, Wesch D, Pitters E, Zöller M. Characterization of tumor reactivity of human V gamma 9V delta 2 gamma delta T cells in vitro and in SCID mice in vivo. *J Immunol*. 2004;173(11):6767–6776.
32. Xiang Z, et al. Targeted activation of human Vγ9Vδ2-T cells controls Epstein-Barr virus-induced B cell lymphoproliferative disease. *Cancer Cell*. 2014;26(4):565–576.
33. Vereide D, Sugden B. Insights into the evolution of lymphomas induced by Epstein-Barr virus. *Adv Cancer Res*. 2010;108:1–19.
34. Ma SD, et al. LMP1-deficient Epstein-Barr virus mutant requires T cells for lymphomagenesis. *J Clin Invest*. 2015;125(1):304–315.
35. Ma SD, et al. PD-1/CTLA-4 blockade inhibits Epstein-Barr virus-induced lymphoma growth in a cord blood humanized-mouse model. *PLoS Pathog*. 2016;12(5):e1005642.
36. Zumwalde NA, et al. Analysis of immune cells from human mammary ductal epithelial organoids reveals Vδ2$^+$ T cells that efficiently target breast carcinoma cells in the presence of bisphosphonate. *Cancer Prev Res (Phila)*. 2016;9(4):305–316.
37. Bukowski JF, Morita CT, Band H, Brenner MB. Crucial role of TCR gamma chain junctional region in prenyl pyrophosphate antigen recognition by gamma delta T cells. *J Immunol*. 1998;161(1):286–293.
38. Bukowski JF, Morita CT, Tanaka Y, Bloom BR, Brenner MB, Band H. V gamma 2V delta 2 TCR-dependent recognition of non-peptide antigens and Daudi cells analyzed by TCR gene transfer. *J Immunol*. 1995;154(3):998–1006.
39. Prabhu SB, et al. Comparison of human neonatal and adult blood leukocyte subset composition phenotypes. *PLoS One*. 2016;11(9):e0162242.
40. Schildberg FA, Klein SR, Freeman GJ, Sharpe AH. Coinhibitory pathways in the B7-CD28 ligand-receptor family. *Immunity*. 2016;44(5):955–972.
41. Leung J, Suh WK. The CD28-B7 family in anti-tumor immunity: emerging concepts in cancer immunotherapy. *Immune Netw*. 2014;14(6):265–276.
42. Tsai MH, et al. Spontaneous lytic replication and epitheliotropism define an Epstein-Barr virus strain found in carcinomas. *Cell Rep*. 2013;5(2):458–470.
43. Brandes M, Willimann K, Moser B. Professional antigen-presentation function by human gammadelta T cells. *Science*. 2005;309(5732):264–268.
44. Landmeier S, et al. Activated human gammadelta T cells as stimulators of specific CD8$^+$ T-cell responses to subdominant Epstein Barr virus epitopes: potential for immunotherapy of cancer. *J Immunother*. 2009;32(3):310–321.
45. Brandes M, et al. Cross-presenting human gammadelta T cells induce robust CD8$^+$ alphabeta T cell responses. *Proc Natl Acad Sci*

U S A. 2009;106(7):2307–2312.
46. Altvater B, et al. Activated human γδ T cells induce peptide-specific CD8+ T-cell responses to tumor-associated self-antigens. *Cancer Immunol Immunother*. 2012;61(3):385–396.
47. Kobayashi H, et al. Safety profile and anti-tumor effects of adoptive immunotherapy using gamma-delta T cells against advanced renal cell carcinoma: a pilot study. *Cancer Immunol Immunother*. 2007;56(4):469–476.
48. Kobayashi H, Tanaka Y, Yagi J, Minato N, Tanabe K. Phase I/II study of adoptive transfer of γδ T cells in combination with zoledronic acid and IL-2 to patients with advanced renal cell carcinoma. *Cancer Immunol Immunother*. 2011;60(8):1075–1084.
49. Nicol AJ, et al. Clinical evaluation of autologous gamma delta T cell-based immunotherapy for metastatic solid tumours. *Br J Cancer*. 2011;105(6):778–786.
50. Wilhelm M, et al. Successful adoptive transfer and in vivo expansion of haploidentical γδ T cells. *J Transl Med*. 2014;12:45.
51. Abe Y, et al. Clinical and immunological evaluation of zoledronate-activated Vgamma9gammadelta T-cell-based immunotherapy for patients with multiple myeloma. *Exp Hematol*. 2009;37(8):956–968.
52. Bennouna J, et al. Phase-I study of Innacell gammadelta, an autologous cell-therapy product highly enriched in gamma9delta2 T lymphocytes, in combination with IL-2, in patients with metastatic renal cell carcinoma. *Cancer Immunol Immunother*. 2008;57(11):1599–1609.
53. Nakajima J, et al. A phase I study of adoptive immunotherapy for recurrent non-small-cell lung cancer patients with autologous gammadelta T cells. *Eur J Cardiothorac Surg*. 2010;37(5):1191–1197.
54. Sakamoto M, et al. Adoptive immunotherapy for advanced non-small cell lung cancer using zoledronate-expanded γδTcells: a phase I clinical study. *J Immunother*. 2011;34(2):202–211.
55. Ma SD, et al. A new model of Epstein-Barr virus infection reveals an important role for early lytic viral protein expression in the development of lymphomas. *J Virol*. 2011;85(1):165–177.
56. Schneider CL, Hudson AW. The human herpesvirus-7 (HHV-7) U21 immunoevasin subverts NK-mediated cytoxicity through modulation of MICA and MICB. *PLoS Pathog*. 2011;7(11):e1002362.

Expansion and Adoptive Transfer of Human Vδ2^{+} T cells to Assess Antitumor Effects *In Vivo*

Akshat Sharma*, Nicholas A. Zumwalde*, Jenny E. Gumperz

Department of Medical Microbiology and Immunology, University of Wisconsin School of Medicine and Public Health, Madison, WI 53706, USA.

* These authors contributed equivalently

Correspondence: Dr. Jenny E. Gumperz **(**jegumperz@wisc.edu)

Key words: humanized mice; γδ T cells; Epstein-Barr virus; lymphoma; tumor immunosuppression; tumor immunosurveillance; tumor immunotherapy

Abstract

Recent clinical trials have yielded promising results suggesting that γδ T cell-based immunotherapies can be effective against hematological malignancies. Human T cells expressing Vγ9Vδ2$^+$ receptors are particularly attractive candidates for this application, since they can be readily expanded *in vitro* in large quantities for adoptive transfer and do not require HLA-matching of donors and recipients. While it is well established that Vγ9Vδ2$^+$ T cells are potently cytolytic against many human cancers and it has been shown that they can control transplanted human tumors in xenogeneic model systems, little is known about the parameters that determine the anti-tumor efficacy of adoptively transferred Vγ9Vδ2$^+$ T cells in physiologically relevant scenarios. In particular, it may be important to separate their immunosurveillance functions from those employed in the context of an established tumor. Moreover, it is critical to understand how the presence of an immunosuppressive environment, such as one where tumor-infiltrating T cells are held in check by inhibitory ligands, affects the functions of Vγ9Vδ2$^+$ T cells. This chapter describes how to establish Epstein-Barr Virus (EBV) infection of human umbilical cord blood mononuclear cells (CBMCs) within immunodeficient mice, so as to drive the *in vivo* formation of human B cell lymphomas that contain an immunosuppressive environment. Details are provided on how to expand human Vγ9Vδ2$^+$ T cells from peripheral blood mononuclear cells (PBMCs), administer them to the mice, and evaluate tumors and other tissues.

1 Introduction

Anti-tumor functions of γδ T cells. Since they were first identified about 30 years ago, it has been clear that human γδ T cells display potent cytotoxicity towards tumor target cells (Moingeon et al. 1986). Human γδ T cells lyse target cells in an MHC-unrestricted manner, and have been shown to efficiently kill a variety of neoplastic cell types, particularly those of hematological and epithelial origin (Ensslin and Formby 1991; Fisch et al. 1990; Sturm et al. 1990). Based on their ability to eradicate primary human tumor cells *in vitro* (Braza et al. 2011; Burjanadze et al. 2007; D'Asaro et al. 2010; Gertner-Dardenne et al. 2012; Kunzmann et al. 2000; Saitoh et al. 2008), and on studies showing that human γδ T cells can control xenografted human tumors in immune-deficient mice *in vivo* (Chen et al. 2001; Kabelitz et al. 2004; Lozupone et al. 2004; Malkovska et al. 1992; Xiang et al. 2014; Zheng et al. 2001), pilot clinical trials have been undertaken to investigate γδ T cell-based immunotherapies in cancer patients (for recent reviews see (Braza and Klein 2013; Fournie et al. 2013)). While the results of these studies have overall been promising (a recent meta-analysis of 13 clinical trials that used γδ T cell-based immunotherapies and involved patients with advanced or metastatic cancer found a total Effective Rate of 0.407 with a p value <0.014 (Buccheri et al. 2014)), the mechanistic pathways used by human γδ T cells to mediate anti-tumor effects *in vivo* remain poorly understood. For example, it is not clear whether their anti-tumor effects are necessarily due to their cytotoxic functions, since a number of studies have suggested that γδ T cells may also promote antigen-specific anti-tumor responses by acting as highly stimulatory antigen presenting cells (APCs) for HLA-restricted T cells (Altvater et al. 2012; Brandes et al. 2009; Brandes et al. 2005; Landmeier et al. 2009). Hence, methodologies that allow for investigation of mechanisms underlying the anti-tumor effects of human γδ T cells *in vivo* are of considerable interest.

EBV model system. To generate a an experimental model for investigating the anti-tumor effects of human γδ T cell adoptive therapy, we have used Epstein-Barr virus (EBV) to drive the *de novo* formation of human B-lymphomas *in vivo*. EBV is a completely human-specific γ-herpesvirus that infects B lymphocytes, causing dysregulated proliferation (Moss et al. 2001). Primary EBV infection is typically controlled by cytolytic lymphocyte responses (Taylor et al. 2015). However, in situations where the initial viral infection is overwhelming or the cytolytic response is sub-optimal, failure to contain the virus leads to potentially fatal B cell proliferation. This is particularly common when pediatric patients who are naive to EBV are transplanted with organs or tissue from an EBV-infected individual; the ensuing pathology is thus termed post-transplant lymphoproliferative disease (PTLD) (Hopwood and Crawford 2000). PTLD is an increasingly common complication after allogeneic stem cell transplantation (Sanz and Andreu 2014).

We have taken advantage of the fact that human umbilical cord blood lymphocytes are naive to EBV to establish an experimental system resembling post-transplant lymphoproliferative disease. By transferring freshly isolated human umbilical cord blood mononuclear cells (CBMCs) and EBV into immunodeficient mice, the initially healthy human B cells become infected by EBV and undergo neoplastic transformation *in vivo* during the ensuing 2-3 weeks. Typically, about 80-90% of the mice will ultimately develop invasive lymphomas within the peritoneal cavity (Ma et al. 2015). The lymphomas are heavily infiltrated by autologous human $CD4^+$ and $CD8^+$ T cells derived from the umbilical cord blood sample (Ma et al. 2015). However, the B cells in the lymphomas express immunosuppressive ligands (e.g. PD-L1, PD-L2) that hold the anti-tumor functions of the T cells in check (Ma et al. 2016). Thus, this model provides the opportunity to evaluate both the immunosurveillance and tumor rejection functions of human γδ T cells. By adoptively transferring human γδ T cells within the first 1-2 weeks after the injection of CBMCs and EBV their impact on virally infected cells that are only nascently

neoplastic can be evaluated (i.e. immunosurveillance). Alternatively, by waiting to administer the γδ T cells until 3-4 weeks, their effects can be evaluated in the context of established tumors containing an immunosuppressive environment (Zumwalde et al. 2017).

Expansion of Vδ2$^+$ T cells from human blood. Human γδ T cells are divided into two main subsets based on their T cell receptor (TCR) usage of the Vδ1 chain or the Vδ2 chain. Most of the γδ T cells in human blood use the Vδ2 chain, which is typically paired with the Vγ9 chain. Nearly all Vδ2$^+$ T cells can be potently activated in a TCR-dependent manner by small chemical compounds comprised of a hydrophobic alkyl moiety linked to a polar group that contains one or more phosphates (Bukowski et al. 1998; Bukowski et al. 1995; Morita et al. 1995; Tanaka et al. 1994). Compounds of this type include prenylpyrophosphate metabolites, such as isopentenylpyrophosphate (IPP). FDA-approved bisphosphonate drugs (e.g. Alendronate, Zoledronate) that are prescribed for the prevention and treatment of osteopenia lead to the potent activation of human Vδ2$^+$ T cells, because they block the mevalonate biosynthesis pathway and cause the accumulation of IPP within cells. While the molecular recognition events are not yet fully resolved, it appears that IPP binds to the cytoplasmic tail of an immunoglobulin-superfamily molecule related to the B7-family, called butyrophilin 3A1 (BTN3A1) (Vavassori et al. 2013; Wang et al. 2013). The association of prenylpyrophosphate molecules with the cytoplasmic tail of BTN3A1 causes a change that is detected at the cell surface by Vδ2$^+$ T cells, leading to their proliferation and induction of effector functions (Decaup et al. 2014; Rhodes et al. 2015; Riano et al. 2014; Sandstrom et al. 2014; Wang and Morita 2015). Exposing human peripheral blood mononuclear cells (PBMCs) to bisphosphonate drugs thus provides a simple means to selectively drive the proliferation and activation of Vδ2$^+$ T cells, so as to produce an expanded population of cells that can be used for cellular immunotherapy.

The following sections provide detailed descriptions of methods for setting up the EBV-driven

lymphoma model in immunodeficient mice, expanding $V\delta2^+$ T cells from human PBMCs, and harvesting and analyzing lymphomas and other tissues from the mice.

2 Materials

2.1 Engraftment of NSG mice with EBV-exposed human umbilical cord blood cells

2.1.1 Preparation of EBV

1. A titered solution of the lytic M81 strain of EBV, stored in frozen aliquots at -80 ^{o}C or in LN_2 (*see* **Note 1**). Virus is stored in 200 μl aliquots,at a concentration of 200 IU/μl. Thus, each vial contains a total of 40,000 IU of virus, which is sufficient for 20 mice (the average number of mice that can be generated from one cord blood sample).

2.1.2. Preparation of human umbilical cord blood cells and exposure to EBV

1. Human umbilical cord blood mononuclear cells (*see* **Note 2**).
2. Ficoll-Paque Premium (GE Healthcare; Pittsburgh, PA).
3. 50 ml conical tubes (sterile).
4. RPMI 1640 medium (keep cold; 2-8°C).
5. Culture Medium: RPMI 1640, 10% bovine calf serum (heat inactivated), 3% human AB serum, 1% L-Glu, 1% Penicillin-Streptomycin.
6. Ammonium-Chloride-Potassium (ACK) lysis buffer (keep cold; 2-8°C).
7. Sterile PBS, tissue culture grade.

2.1.3 Injection of EBV-treated CBMCs into immunodeficient mice

1. 6-8 week old NOD.Cg-Prkdc^{scid}Il2rg^{tm1Wjl}/SzJ (NSG) mice (Jackson Labs).
2. Tuberculin syringes and 28.5 gauge needles.

2.2 Expansion of Vδ2^{+} T cells from adult peripheral blood and adoptive transfer into EBV-infected mice

2.2.1 Expansion of human Vδ2^{+} T cells

1. Anticoagulant treated peripheral blood obtained from healthy adult donors after informed consent, or purified peripheral blood mononuclear cells (PBMCs).
2. Ficoll-Paque PLUS (GE Healthcare; Pittsburgh, PA).

3. T cell culture medium: RPMI-1640, 15% bovine calf serum (heat inactivated), 3% human AB serum, 1% L-Glu, 1% Penicillin-Streptomycin, 200 U/mL interleukin-2 (IL-2).

4. Zometa (zoledronic acid; Novartis).

5. Antibodies to assess expansion and purity of γδ T cells, such as: anti-Vδ2 (clone B6; BioLegend), anti-Vγ9 (clone B3; BioLegend), anti-CD3 (clones OKT3 or HIT3a; BioLegend)

6. Flow cytometer for analysis of expanded γδ T cells.

7. Freezing solution (15% DMSO in bovine calf serum) and cryovials.

2.2.2 Adoptive transfer of human Vδ2$^+$ T cells

1. Sterile PBS, tissue culture grade.

2. Tuberculin syringes and 28.5 gauge needles.

3. Isoflurane and isoflurane chamber for mouse anesthesia

2.3 Collection and analysis of tumors and spleen tissue

2.3.1 Harvesting tumor and spleen tissue

1. Forceps.

2. Surgical scissors.

3. Surgical foam board.

4. Pins.

2.3.2 Determining tumor burden and preparing tissues for further analysis

1. 50 ml conical tubes, pre-weighed.

2. Scale.

3. 10% Formalin solution, neutral buffered.

4. Filter mesh and plungers for manual dissociation of tissues, or gentleMACS dissociator (Miltenyi Biotec).

5. PBS

2.3.3 Histological analysis of tissues

1. Biopsy/embedding cassettes.
2. Absolute ethanol and solutions of 70% and 90% ethanol.
3. Xylene.
4. Forceps.
5. Scissors.
6. Base molds.
7. Heating block.
8. Paraffin wax.

2.3.4 Flow cytometric analysis of spleen or tumor tissues

1. Fc blocking solution consisting of 20% human AB serum in PBS.
2. Tubes appropriate for reading samples on flow cytometer.
3. Flow cytometry sample buffer consisting of a filtered solution of 1 mg/ml BSA in PBS.
4. Flow cytometer capable of detecting at least 4 channels (preferably 8 or 9).
5. Antibodies for human cell markers: anti-CD45 (clone HI30; BioLegend), anti-pan HLA-A,B,C (clone W6/32; BioLegend), anti-CD3 (clone OKT3 or HIT3a; BioLegend), anti-CD19 (clone SJ25C1; BioLegend) or anti-CD20 (clone 2H7; BioLegend), anti-Vδ2 (clone B6; BioLegend) or anti-Vγ9 (clone B3; BioLegend). Antibodies against CD19 and CD20 can be used in the same color improve detection of EBV-infected B cells.

3 Methods

3.1 Engraftment of NSG mice with EBV-exposed human umbilical cord blood cells

3.1.1 Preparation of EBV

1. Thaw sufficient virus for the experiment by briefly incubating one or more frozen aliquots at 37 ^{o}C. (Typically, 200 IU of virus is used per 1 x 10^6 CBMCs and each mouse is injected with 10 x 10^6 CBMCs, although these numbers may vary depending on the activity of the virus and the availability of CBMCs.)

3.1.2 Preparation of human umbilical cord blood cells and exposure to EBV

1. If frozen purified CBMCs are used, thaw the cells and wash them according to the supplier's instructions, then resuspend at 1 x 10^8 cells/ml in culture medium. If whole cord blood is used, the CBMCs must first be isolated by density gradient centrifugation.

2. Dilute the whole cord blood with 3x the volume of cold RPMI, and place 35 ml each into 50 ml conical tubes. Slowly pipet 15ml of the Ficoll-Paque under 35 ml of the diluted cord blood.

3. Centrifuge at 400xg for 40-45 minutes in a centrifuge with a swinging bucket rotor without using brakes or acceleration.

4. After centrifugation, the blood will have separated into layers: plasma (clear top layer), CBMCs (cloudy or opaque layer at top of interface with Ficoll), dark red bottom layer containing granulocytes and erythrocytes. Aspirate the plasma layer without disturbing the CBMCs, and discard.

5. Gently aspirate the CBMCs and transfer into a fresh 50 ml conical tube.

6. Fill the CBMC-containing conical tube with RPMI, and centrifuge at 400xg for 15 min at 18°C with full acceleration and brake.

7. Discard the supernatant, resuspend the CBMC pellet in RPMI and spin at 300xg for 15 min at 18°C with full acceleration and brake.

8. Repeat step 7, but at 200xg. The spins described in steps 6-8 help remove platelets from CMBC.

9. If the CBMC appears red it likely has significant erythrocyte contamination. In this case, resuspend in 10-15 ml of cold ACK lysis buffer and incubate for 5 mins at room temperature. Lysis of erythrocytes should be evident by this time. Fill the tube with culture medium to dilute out the ACK lysis buffer, and spin the cells down at 300xg for 15 minutes.

10. Resuspend the CBMC pellet in 1.5-2ml culture medium, and count the cells. Dilute to 1 x 10^8 cells/ml in culture medium.

11. Add 2000 IU of M81 per 1 x 10^7 CBMC and incubate at 37°C, 5% CO2, for 2-4 hours, to

promote viral attachment to the B lymphocytes in the CBMC sample.

12. Wash the CMBC with culture medium to remove non-attached virions. Resuspend in sterile PBS (room temperature) at a concentration of $5x10^7$ cells per ml.

3.1.3 Injection of EBV-treated CBMCs into immunodeficient mice

1. Using sterile tuberculin syringes and 28.5 gauge needles, intraperitoneally inject 200 μl of the cell suspension (1×10^7 CBMC) per mouse.

2. Mice should be maintained in a specific pathogen-free facility using sterilized cages, bedding, food, and water. Tumors will form in the peritoneal cavity by about 21 days post-injection of EBV-exposed CBMCs; γδ T cell treatment can be performed at any time point depending on whether the goal is to investigate immunosurveillance functions (i.e. prevention of neoplastic cell outgrowth or tumor deposition), or effects that occur in the presence of established tumors (e.g. infiltration or eradication).

3.2 Expansion of Vδ2$^+$ T cells from adult peripheral blood and adoptive transfer into EBV-infected mice

3.2.1 Expansion of human Vδ2$^+$ T cells

1. If frozen purified PBMCs are used, thaw the cells and wash them according to the supplier's instructions, then resuspend at $2x10^6$ cells/ml in T cell culture medium. If whole peripheral blood is used, the PBMCs must first be isolated by density gradient centrifugation using Ficoll-PLUS, as described for CBMCs in section 3.1.2.

1. Dilute Zometa to a concentration of 5 μM in T cell culture medium.

2. Add equal volumes of PBMCs (0.5 ml) and 5 μM Zometa (0.5 ml) to wells of a 24-well plate, resulting in a density of $1x10^6$ cells/well and a final Zometa concentration of 2.5 μM (*see* **Note 3**).

3. Incubate the cells at 37 °C in a humidified incubator with 5% CO_2.

4. Monitor the cultures to assess cell growth and acidification of the culture medium. Add 1 ml fresh T cell culture medium after 4-6 days, or sooner if the wells appear to be turning orange or yellow. As the cells expand (typically in the second week of culture), split each well into a second well and supplement with fresh T cell culture media.

5. Flow cytometric analyses should be performed to assess purity of γδ T cells and expression of ligands of interest (e.g. PD-1). (*see* **Note 4**).

6. Cultures containing expanded Vδ2$^+$ T cells are typically harvested after 8-14 days, with the precise timing chosen according to the level of Vδ2$^+$ T cell enrichment and total cell number. If necessary, contaminating cell types can be removed from the expanded Vδ2$^+$ T cell culture by magnetic or flow cytometric sorting. (*see* **Note 5**).

7. The can also be stored frozen for up to 3 months prior to use. Chill a suspension of culture medium containing 2-10 x 10^7 cells/ml and mix with 2x volume of cold freezing solution (15% DMSO in bovine calf serum). Pipet into pre-chilled cryovials and immediately transfer to -80 ^{o}C.

3.2.2 Adoptive transfer of human Vδ2$^+$ T cells

1. If the expanded γδ T cells have been stored frozen, thaw and wash cells several times with sterile PBS to remove DMSO.

2. Count cells and resuspend at 2.5x10^7 cells/ml in sterile PBS.

3. Anesthetize mice that were injected with EBV-exposed CBMCs.

4. Intravenously administer 2.5-5x10^7 cells in a volume of 100-200 μl by retro-orbital injection. Control mice should be injected with an equivalent volume of sterile PBS.

3.3 Collection and analysis of tumors and spleen tissue

3.3.1 Harvesting tumor and spleen tissue

1. Tumors are typically visible in the peritoneal cavity by 21 days post-injection of EBV-exposed CBMCs; mice typically become moribund by about 32-34 days post-injection. Thus, analyses can be done at any time during this window.

2. Euthanize the mice as specified by your institutional Animal Care and Use Committee.

3. Place murine carcasses with the ventral side up on a surgical foam board, and pin the limbs to the board.

4. Using a pair of forceps, pull the skin near the urethral opening upwards, and make an incision with a pair of surgical scissors. The incision should cut along the midline, and go from the urethral opening up to the chin.

5. Using the forceps carefully pinch the peritoneal sac pulling upwards and making an incision identical to the one in step 4 to expose the viscera.

6. Tumors are most commonly found initially in peri-pancreatic areas, and at later stages often invade pancreas, bile duct, liver, intestines, and (less commonly) other tissues. Locate the stomach on the left side of the peritoneal cavity, and with a pair of forceps, begin to separate the pancreas from the stomach and the intestines, delicately severing connections between the pancreas and the thorax using either another pair of forceps or a pair of surgical scissors.

7. Pull out the spleen and attached pancreas, and separate the spleen. Spleens should be weighed and then placed into cold culture medium or fixative solution for later analysis (e.g. flow cytometry or histology).

8. Place the pancreas and any associated tissue on the surgical foam board to examine for the presence of tumors. The mesenteric tissue wrapped around the pancreas can often be infiltrated with tumors or lymphoid aggregates giving it a bulbous, engorged appearance. Thus, while the pancreas itself is shaped like a flat pear with pink coloration (sometimes grey-ish when infiltrated by tumor cells), the tumors are usually lighter-colored masses with a firm texture. Carefully dissect the tumor tissue from the pancreas (*see* **Figure 1A and B**).

9. Using a pair of forceps, also examine the mesentery, stomach, intestine and liver lobes for tumors. These will appear as white/pinkish engorged masses resting on the tissue, and can be harvested using scissors.

3.3.2 Determining tumor burden and preparing tissues for further analysis

1. Decide whether tumors will be analyzed by histology or flow cytometry, and prepare 50 ml conical tubes with 5-10 ml 10% neutral buffered formalin (histology) or cold culture medium (flow cytometry). Weigh the tubes containing the appropriate buffer, and record the weight on the side of the tube. To determine the tumor burden, place all of the excised tumor tissue from an individual mouse into a tube, and re-weigh using the same scale. Subtract the tube weight to obtain the weight of the tumor tissue.

2. Tissues collected for histology may be stored at room temperature in 10% neutral buffered formalin for 24-48h, before further processing.

3. Tissues that are to be analyzed by flow cytometry should be kept cold and processed immediately.

3.3.3 Histological analysis of fixed tissues

1. To prepare them for paraffin sectioning, cut the tissue into slices ~3mm thick. Tissue preparation is often performed by a core facility or a commercial service using an automated tissue processor. Alternatively, processing steps can be completed manually as described briefly in the following steps (Slaoui and Fiette 2011).

2. Place the tissues into appropriately labeled embedding cassettes. Put the cassettes in a beaker containing 70% ethanol, and incubate at room temperature for 60 min.

3. Transfer the cassettes to a beaker of 95% ethanol, and incubate for 60 min.

4. Transfer the cassettes to a beaker of absolute ethanol, and incubate for 60 min. Repeat twice.

5. Transfer the cassettes to a beaker containing xylene, and incubate for 20 min. Repeat twice, with the final incubation lasting 45 min to 24 hr.

6. Place cassettes in a container of molten paraffin wax and agitate gently for 30 min. Repeat twice.

7. Fill block molds with molten paraffin wax and position tissue within the wax as desired for sectioning; place cassette on top as backing.

8. Tissue can now be sectioned using a microtome and placed onto slides. For each tissue, it is helpful to perform hematoxylin and eosin staining on the first slide of a series of serial sections to identify areas of interest (e.g. tissues containing lymphocytes that likely correspond to tumor or lymphoid tissue). Further serial sections can then be chosen and immunohistochemistry performed using specific antibodies, as described (Lockridge et al. 2013; Ma et al. 2011; Ma et al. 2016; Ma et al. 2015; Ma et al. 2012; Zumwalde et al. 2017).

3.3.4 Flow cytometric analysis of spleen or tumor tissues

1. Prepare a single cell suspension from the tissue sample. Tissues can be dissociated manually by using the backside of a plunger from a plastic syringe to mash the tissue over filter mesh (40-100 μm), or automatically using a tissue dissociator. If desired, the single cell suspension can be stored frozen using the freezing procedure described in step 7 of section 3.2.1..

2. Centrifuge samples at 400xg for 5 minutes to pellet cells, and discard supernatant.

3. Resuspend in PBS and pass through a 40-100 μm filter mesh (*see* **Note 6**).

4. Suspend single cell suspension in 1 ml Fc-blocking buffer and incubate for 15 minutes at 4 ^{o}C.

5. Pellet cells by centrifugation and pour off supernatant.

6. Add cocktail of staining antibodies to the void volume in the tubes and incubate for 30 minutes at 4 °C.

7. Wash the samples with flow cytometry sample buffer, and resuspend in a volume of 0.3-0.5 ml.

8. Analyze samples on flow cytometer (*see* **Notes 7-9**).

4 Notes

1. We recommend using a lytic strain of EBV (e.g. M81, Akata) rather than the more commonly used B95-8 strain. B95-8 lacks EBV-encoded microRNAs and has an almost completely latent pattern of gene expression, whereas strains such as M81 contain the whole viral genome and show both lytic and latent gene expression. Since most of the EBV peptide epitopes recognized by $CD8^+$ T cells derive from lytic genes, the use of a lytic strain produces better virally-driven $CD8^+$ T cell expansion and thus also provides for better modeling of the immunosuppressive environment that can thwart anti-tumor T cell responses.

   The titer of the virus particles must established prior to use. To do this, we make use of an EBV construct that expresses the green fluorescent protein (GFP) (Tsai et al. 2013). Infectious viral particles are produced from 293 cell lines that were stably infected with the M81 strain of EBV following transfection with EBV BZLF1 expression vector as described (Ma et al. 2011). The titer of infectious EBV is determined by assessing the number of fluorescent Raji cells derived from serial dilutions of the concentrated virus stock and calculating the green Raji unit (GRU) titer, as described (Ma et al. 2011).

2. Cord blood may be obtained as an anticoagulant-treated whole blood sample, or as purified cord blood mononuclear cells (CBMCs) that are supplied either fresh or frozen. The $CD34^+$ cells are not needed for this protocol, and so if desired these may be removed from the CBMCs by magnetic sorting prior to EBV-exposure.

3. In Zometa expanded PBMC cultures, $V\delta2^+$ T cells typically comprise 70-80% of the total CD3 population between days 7 and 11 post stimulation. However, the percentage of $V\delta2^+$ T cells can vary depending on the initial frequency of $\gamma\delta$ T cells in the starting PBMC sample and the potency of the Zometa preparation, among other variables. It is therefore advisable to monitor the $V\delta2^+$ T cell expansion using flow cytometry, by testing the starting PBMCs at day 0, and on the day of harvest.

4. In the Zometa expanded $V\delta2^+$ T cell cultures, we have observed that PD-1 becomes transiently upregulated, typically peaking at about day 4, then returns to baseline by day 6-8 and remains low for the subsequent days of culture. Remarkably, the $V\delta2^+$ T cells maintain their low PD-1 expression after adoptive transfer (Zumwalde et al. 2017). Since low cell surface expression of PD-1 may be important for the anti-tumor functions of the adoptively transferred $V\delta2^+$ T cells, we recommend that flow analyses be performed to confirm that the transient elevation of PD-1 expression has subsided, prior to adoptive transfer.

5. We have not seen evidence that contaminating cell types in cultures of Zometa-expanded $V\delta2^+$ T cells have an impact on anti-tumor effects (Zumwalde et al. 2017). However, if desired, further sorting can be performed to increase $V\delta2^+$ T cell purity. Since most of the contaminating cells are usually $\alpha\beta$ T cells, negative selection can be performed using pan-$\alpha\beta$ TCR antibodies. However, since other populations (e.g. NK cells) are sometimes also present at low frequencies in the culture, if an essentially 100% pure population of $V\delta2^+$ T cells is desired, it may be necessary to positively select the $V\delta2^+$ T cells using an antibody against $V\delta2$ or $V\gamma9$. Importantly, we have not validated whether such positive selection using reagents that bind the TCR impacts the functioning of the $V\delta2^+$ T cells after adoptive transfer.

6. The viability of cells from tumor samples is often much lower than that of spleen samples. Tumor samples typically also require additional filtering compared to the spleen.

7. Detection and analysis of human cells requires careful flow cytometric gating. It is helpful to set a singlets gate using side-scatter parameters, then gate on FSC vs. SSC to focus on live cells (*see* **Figure 2A**). It is best to use at least two different parameters to identify the total human cell population, such as pan-HLA-A,B,C staining and anti-human CD45. Murine cells can also be excluded using antibodies against H-2, CD45, or other widely distributed murine antigens. Human cells identified by pan-HLA-A,B,C and anti-CD45 typically distribute into two nodes (*see* **Figure 2B**), with the HLA-A,B,C^{bright}/$CD45^{intermediate}$ population corresponding to B lymphocytes and the HLA-A,B,$C^{intermediate}$/$CD45^{bright}$ subset corresponding to T lymphocytes. The EBV-infected B lymphocytes often down-regulate CD20, and to a lesser extent CD19, from the cell surface at later stages in the infection. Thus, it can be helpful to stain for both of these markers in the same channel to amplify the signal. Nevertheless, even though histological analyses of the same tissue sample typically reveal abundant $CD20^{+}$ cells, flow cytometric staining often reveals a distribution of CD3-negative human cells that range from clearly CD19/CD20 positive to essentially negative (*see* **Figure 2C**).

   To accurately gauge expression of critical markers or to identify potentially rare cell types (e.g. adoptively transferred γδ T cells), it is helpful to set up parallel "fluorescence-minus-one" negative control samples, that are stained with all of the antibodies except the one of interest.

8. When staining for the adoptively transferred Vγ9Vδ2 T cells, it is best to use just a single TCR-specific reagent, since staining is often sub-optimal if multiple TCR-binding reagents (e.g. anti-Vγ9, anti-Vδ2, and anti-pan γδ mAbs) are all used in the same staining panel.

9. If delineating the adoptively transferred γδ T cells from those of the cord blood sample is important, HLA-A2 mismatching is helpful (Zumwalde et al. 2017). This is accomplished by staining CBMC and PBMC samples in order to identify samples that are mis-matched in regards to expression of HLA-A2 using an HLA-A2 specific antibody (clone BB7.2; BioLegend). After the HLA-A2 mis-matched γδ T cells are adoptively transferred, they can be readily distinguished from human cells that are derived from the cord blood sample by including the HLA-A2-specific antibody in the analysis panel.

Acknowledgements

Funding provided by a pilot grant from the University of Wisconsin Carbone Cancer Center that was supported in part by NIH grant NCI P30 CA014520, and by NIH grant R21 AI116007 and DoD CDMRP Award CA160396 to JEG; support for NAZ provided by T32 CA157322. The funders had no role in study design, data collection and analysis, decision to publish, or preparation of the manuscript. The authors have no conflicting financial interests.

References

Altvater B, Pscherer S, Landmeier S, Kailayangiri S, Savoldo B, Juergens H, Rossig C (2012) Activated human gammadelta T cells induce peptide-specific CD8+ T-cell responses to tumor-associated self-antigens Cancer Immunol Immunother 61:385-396 doi:10.1007/s00262-011-1111-6

Brandes M et al. (2009) Cross-presenting human gammadelta T cells induce robust CD8+ alphabeta T cell responses Proceedings of the National Academy of Sciences of the United States of America 106:2307-2312 doi:10.1073/pnas.0810059106

Brandes M, Willimann K, Moser B (2005) Professional antigen-presentation function by human gammadelta T Cells Science 309:264-268 doi:10.1126/science.1110267

Braza MS, Klein B (2013) Anti-tumour immunotherapy with Vgamma9Vdelta2 T lymphocytes: from the bench to the bedside Br J Haematol 160:123-132 doi:10.1111/bjh.12090

Braza MS, Klein B, Fiol G, Rossi JF (2011) gammadelta T-cell killing of primary follicular lymphoma cells is dramatically potentiated by GA101, a type II glycoengineered anti-CD20 monoclonal antibody Haematologica 96:400-407 doi:10.3324/haematol.2010.029520

Buccheri S, Guggino G, Caccamo N, Li Donni P, Dieli F (2014) Efficacy and safety of gammadeltaT cell-based tumor immunotherapy: a meta-analysis Journal of biological regulators and homeostatic agents 28:81-90

Bukowski JF, Morita CT, Band H, Brenner MB (1998) Crucial role of TCR gamma chain junctional region in prenyl pyrophosphate antigen recognition by gamma delta T cells J Immunol 161:286-293.

Bukowski JF, Morita CT, Tanaka Y, Bloom BR, Brenner MB, Band H (1995) V gamma 2V delta 2 TCR-dependent recognition of non-peptide antigens and Daudi cells analyzed by TCR gene transfer J Immunol 154:998-1006

Burjanadze M et al. (2007) In vitro expansion of gamma delta T cells with anti-myeloma cell activity by Phosphostim and IL-2 in patients with multiple myeloma Br J Haematol 139:206-216 doi:10.1111/j.1365-2141.2007.06754.x

Chen J, Niu H, He W, Ba D (2001) Antitumor activity of expanded human tumor-infiltrating gammadelta T lymphocytes Int Arch Allergy Immunol 125:256-263 doi:53824

D'Asaro M et al. (2010) V gamma 9V delta 2 T lymphocytes efficiently recognize and kill zoledronate-sensitized, imatinib-sensitive, and imatinib-resistant chronic myelogenous leukemia cells J Immunol 184:3260-3268 doi:10.4049/jimmunol.0903454

Decaup E, Duault C, Bezombes C, Poupot M, Savina A, Olive D, Fournie JJ (2014) Phosphoantigens and butyrophilin 3A1 induce similar intracellular activation signaling in human TCRVgamma9+ gammadelta T lymphocytes Immunol Letters 161:133-137 doi:10.1016/j.imlet.2014.05.011

Ensslin AS, Formby B (1991) Comparison of cytolytic and proliferative activities of human gamma delta and alpha beta T cells from peripheral blood against various human tumor cell lines Journal of the National Cancer Institute 83:1564-1569

Fisch P et al. (1990) Gamma/delta T cell clones and natural killer cell clones mediate distinct patterns of non-major histocompatibility complex-restricted cytolysis J Exp Med 171:1567-1579

Fournie JJ et al. (2013) What lessons can be learned from gammadelta T cell-based cancer immunotherapy trials? Cell Mol Immunol 10:35-41 doi:10.1038/cmi.2012.39

Gertner-Dardenne J et al. (2012) Human Vgamma9Vdelta2 T cells specifically recognize and kill acute myeloid leukemic blasts J Immunol 188:4701-4708 doi:10.4049/jimmunol.1103710

Hopwood P, Crawford DH (2000) The role of EBV in post-transplant malignancies: a review J Clin Pathol 53:248-254

Kabelitz D, Wesch D, Pitters E, Zoller M (2004) Characterization of tumor reactivity of human V gamma 9V delta 2 gamma delta T cells in vitro and in SCID mice in vivo J Immunol 173:6767-6776

Kunzmann V, Bauer E, Feurle J, Weissinger F, Tony HP, Wilhelm M (2000) Stimulation of gammadelta T cells by aminobisphosphonates and induction of antiplasma cell activity in multiple myeloma Blood 96:384-392

Landmeier S et al. (2009) Activated human gammadelta T cells as stimulators of specific CD8+ T-cell responses to subdominant Epstein Barr virus epitopes: potential for immunotherapy of cancer J Immunother 32:310-321 doi:10.1097/CJI.0b013e31819b7c30

Lockridge JL et al. (2013) Mice Engrafted with Human Fetal Thymic Tissue and Hematopoietic Stem Cells Develop Pathology Resembling Chronic Graft-versus-Host Disease Biol Blood Marrow Transplant doi:10.1016/j.bbmt.2013.06.007

Lozupone F et al. (2004) Effect of human natural killer and gammadelta T cells on the growth of human autologous melanoma xenografts in SCID mice Cancer Res 64:378-385

Ma SD et al. (2011) A new model of Epstein-Barr virus infection reveals an important role for early lytic viral protein expression in the development of lymphomas J Virol 85:165-177 doi:10.1128/JVI.01512-10

Ma SD et al. (2016) PD-1/CTLA-4 Blockade Inhibits Epstein-Barr Virus-Induced Lymphoma Growth in a Cord Blood Humanized-Mouse Model PLoS Pathog 12:e1005642 doi:10.1371/journal.ppat.1005642

Ma SD et al. (2015) LMP1-deficient Epstein-Barr virus mutant requires T cells for lymphomagenesis J Clin Invest 125:304-315 doi:10.1172/JCI76357

Ma SD et al. (2012) An Epstein-Barr Virus (EBV) Mutant with Enhanced BZLF1 Expression Causes Lymphomas with Abortive Lytic EBV Infection in a Humanized Mouse Model J Virol 86:7976-7987 doi:10.1128/JVI.00770-12

Malkovska V, Cigel FK, Armstrong N, Storer BE, Hong R (1992) Antilymphoma activity of human gamma delta T-cells in mice with severe combined immune deficiency Cancer Res 52:5610-5616

Moingeon P et al. (1986) A unique T-cell receptor complex expressed on human fetal lymphocytes displaying natural-killer-like activity Nature 323:638-640 doi:10.1038/323638a0

Morita CT et al. (1995) Direct presentation of nonpeptide prenyl pyrophosphate antigens to human gamma delta T cells Immunity 3:495-507

Moss DJ, Burrows SR, Silins SL, Misko I, Khanna R (2001) The immunology of Epstein-Barr virus infection Philos Trans R Soc Lond B Biol Sci 356:475-488

Rhodes DA et al. (2015) Activation of human gammadelta T cells by cytosolic interactions of BTN3A1 with soluble phosphoantigens and the cytoskeletal adaptor periplakin J Immunol 194:2390-2398 doi:10.4049/jimmunol.1401064

Riano F et al. (2014) Vgamma9Vdelta2 TCR-activation by phosphorylated antigens requires butyrophilin 3 A1 (BTN3A1) and additional genes on human chromosome 6 Eur J Immunol 44:2571-2576 doi:10.1002/eji.201444712

Saitoh A et al. (2008) Anti-tumor cytotoxicity of gammadelta T cells expanded from peripheral blood cells of patients with myeloma and lymphoma Medical oncology 25:137-147 doi:10.1007/s12032-007-9004-4

Sandstrom A et al. (2014) The intracellular B30.2 domain of butyrophilin 3A1 binds phosphoantigens to mediate activation of human Vgamma9Vdelta2 T cells Immunity 40:490-500 doi:10.1016/j.immuni.2014.03.003

Sanz J, Andreu R (2014) Epstein-Barr virus-associated posttransplant lymphoproliferative disorder after allogeneic stem cell transplantation Curr Opin Oncol 26:677-683 doi:10.1097/CCO.0000000000000119

Slaoui M, Fiette L (2011) Histopathology procedures: from tissue sampling to histopathological evaluation Methods Mol Biol 691:69-82 doi:10.1007/978-1-60761-849-2_4

Sturm E, Braakman E, Fisch P, Vreugdenhil RJ, Sondel P, Bolhuis RL (1990) Human V gamma 9-V delta 2 T cell receptor-gamma delta lymphocytes show specificity to Daudi Burkitt's lymphoma cells J Immunol 145:3202-3208

Tanaka Y et al. (1994) Nonpeptide ligands for human gamma delta T cells Proc Natl Acad Sci U S A 91:8175-8179

Taylor GS, Long HM, Brooks JM, Rickinson AB, Hislop AD (2015) The immunology of Epstein-Barr virus-induced disease Annu Rev Immunol 33:787-821 doi:10.1146/annurev-immunol-032414-112326

Tsai MH et al. (2013) Spontaneous lytic replication and epitheliotropism define an Epstein-Barr virus strain found in carcinomas Cell Rep 5:458-470 doi:10.1016/j.celrep.2013.09.012

Vavassori S et al. (2013) Butyrophilin 3A1 binds phosphorylated antigens and stimulates human gammadelta T cells Nat Immunol 14:908-916 doi:10.1038/ni.2665

Wang H et al. (2013) Butyrophilin 3A1 plays an essential role in prenyl pyrophosphate stimulation of human Vgamma2Vdelta2 T cells J Immunol 191:1029-1042 doi:10.4049/jimmunol.1300658

Wang H, Morita CT (2015) Sensor Function for Butyrophilin 3A1 in Prenyl Pyrophosphate Stimulation of Human Vgamma2Vdelta2 T Cells J Immunol 195:4583-4594 doi:10.4049/jimmunol.1500314

Xiang Z et al. (2014) Targeted activation of human Vgamma9Vdelta2-T cells controls epstein-barr virus-induced B cell lymphoproliferative disease Cancer cell 26:565-576 doi:10.1016/j.ccr.2014.07.026

Zheng BJ et al. (2001) Anti-tumor effects of human peripheral gammadelta T cells in a mouse tumor model International journal of cancer Journal international du cancer 92:421-425

Zumwalde NA et al. (2017) Adoptively transferred Vgamma9Vdelta2 T cells show potent antitumor effects in a preclinical B cell lymphomagenesis model JCI Insight 2 doi:10.1172/jci.insight.93179

Figure 1

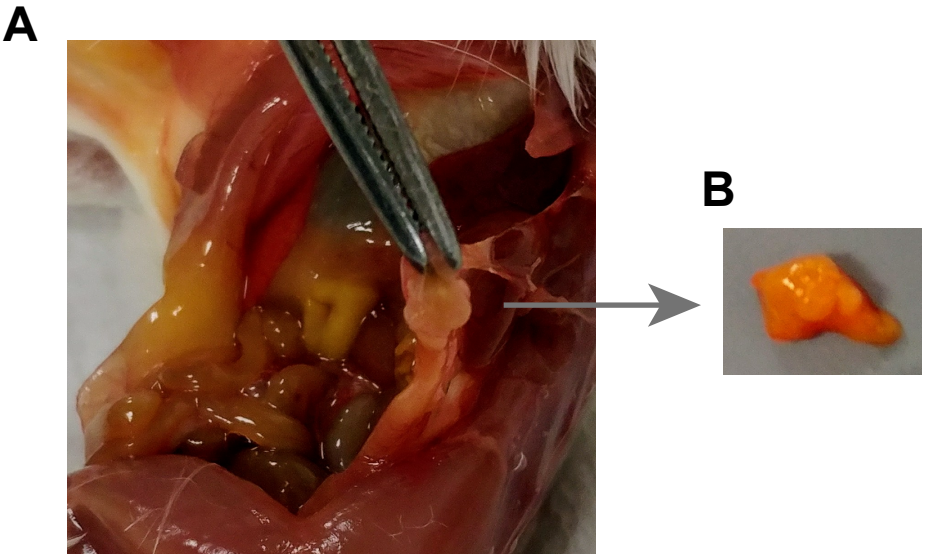

Figure 2

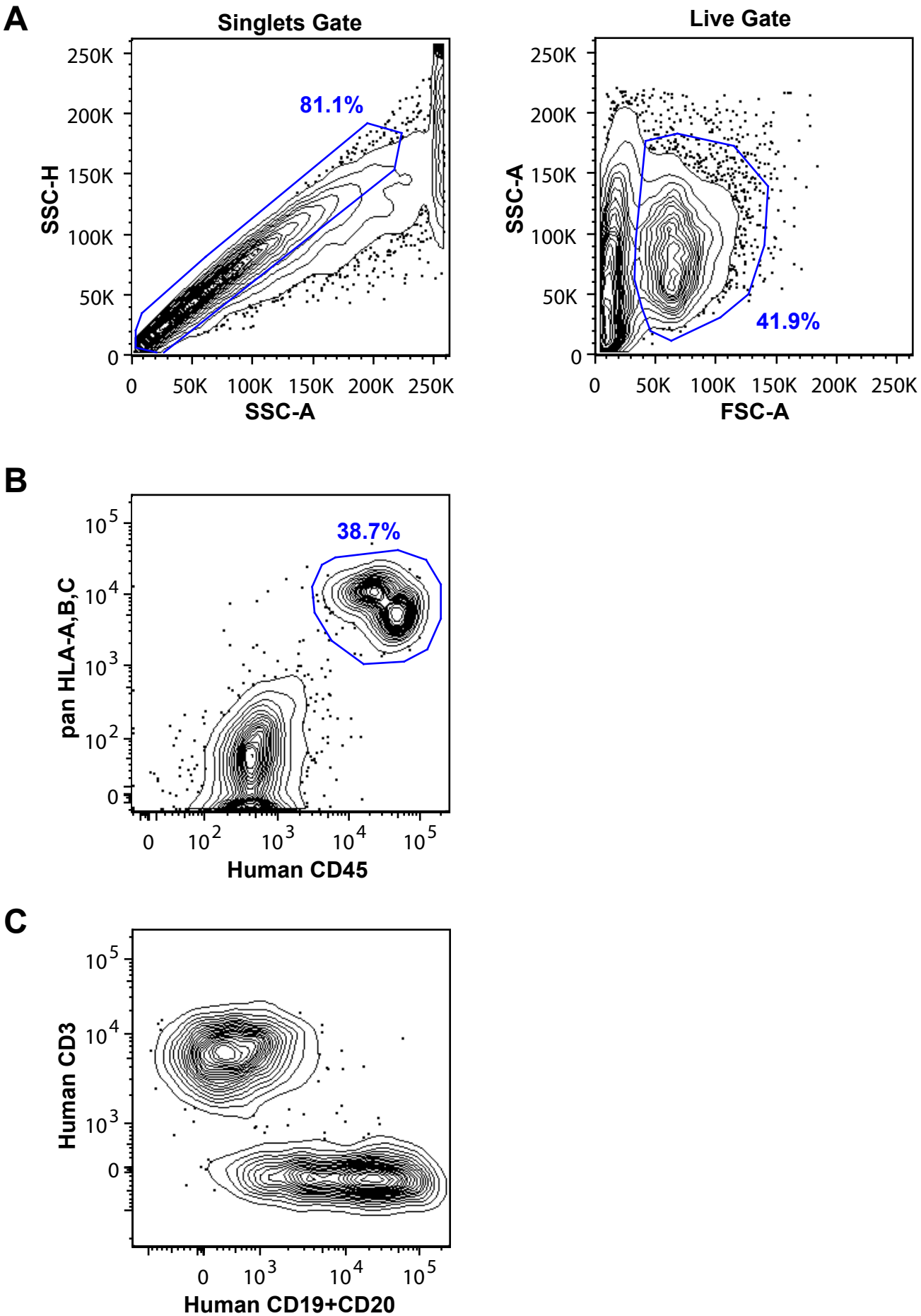
A
Singlets Gate
81.1%
SSC-H
SSC-A
250K
200K
150K
100K
50K
0
Live Gate
41.9%
FSC-A
B
38.7%
pan HLA-A,B,C
Human CD45
C
Human CD3
Human CD19+CD20